Neutral Ruthenium Carbene Complexes bearing N,N,O Heteroscorpionate Ligands: Syntheses and Activity in Metathesis Reactions

Henning Kopf,[†] Bastian Holzberger,[†] Cezary Pietraszuk,[‡] Eike Hübner,[§] and Nicolai Burzlaff*[,§]

Department of Chemistry, Universität Konstanz, Fach M728, D-78457 Konstanz, Germany, Faculty of Chemistry, Adam Mickiewicz University, Grunwaldzka 6, 60-780 Poznań, Poland, and Inorganic Chemistry, Department of Chemistry and Pharmacy & Interdisciplinary Center for Molecular Materials (ICMM), Friedrich-Alexander-University Erlangen-Nürnberg, Egerlandstrasse 1, D-91058 Erlangen, Germany

Received June 30, 2008

Neutral Fischer-type ruthenium(II) aminocarbene complexes bearing the bis(3,5-dimethylpyrazol-1-yl)acetato (bdmpza) ligand have been synthesized by addition of ammonia or methylamine to the α-carbon atom of vinylidene and allenylidene complexes. Reaction with dimethylamine was not successful. These differences in the chemical behavior can be explained by the intermediate formation of intramolecular hydrogen bridges that have been indicated by DFT calculations. Furthermore, octahedral ruthenium(II) benzylidene complexes with the bis(pyrazol-1-yl)acetato (bpza) and the bdmpza ligand were obtained by reacting $[RuCl_2(=CHPh)(PR_3)_2]$ (R = Cy, Ph) with K[bpza] or K[bdmpza], respectively. The latter complexes have successfully been tested for RCM reactions.

Introduction

Ruthenium complexes bearing tridentate ligands have been subjected to many investigations in the past. Beside complexes with the widely spread hydridotris(pyrazol-1-yl)borate ($HB(pz)_3^-$; Tp) ligand,[1] several ruthenium complexes bearing the bis(3,5-dimethylpyrazol-1-yl)acetato (bdmpza) ligand have been published recently[3−5] since this new class of tripod ligands has been introduced to coordination chemistry by Otero in 1999.[2]These facial binding bpza and bdmpza ligands consist of two identical nitrogen donors with σ donor/π acceptor properties and one anionic carboxylate σ donor. Thus, in contrast to κ^3 binding Tp ligands with three identical nitrogen donors, rather different *trans* influences are to be expected in transition metal complexes thereof. Various ruthenium carbene, vinylidene, and allenylidene complexes bearing the Tp[6−9] or bdmpza[10] ligands but also other ligands such as PNP (PNP = N(^{n}Pr)-

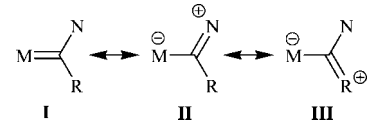

Figure 1. Mesomeric structures of Fischer-type aminocarbene complexes.

* Corresponding author. Tel: (internat.) +49(0)9131/85-28976. Fax: (internat.) +49(0)9131/85-27387. E-mail: burzlaff@chemie.uni-erlangen.de.
† Universität Konstanz.
‡ Adam Mickiewicz University.
§ Friedrich-Alexander-University Erlangen-Nürnberg.

(1) (a) Slugovc, C.; Mereiter, K.; Zobetz, E.; Schmid, R.; Kirchner, K. *Organometallics* **1996**, *15*, 5275–5277. (b) Gemel, C.; Wiede, P.; Mereiter, K.; Sapunov, V. N.; Schmid, R.; Kirchner, K. *J. Chem. Soc., Dalton Trans.* **1996**, 4071–4076. (c) Corrochano, A. E.; Jalón, F. A.; Otero, A.; Kubicki, M. M.; Richard, P. *Organometallics* **1997**, *16*, 145–148. (d) Chen, Y.-Z.; Chan, W. C.; Lau, C. P.; Chu, H. S.; Lee, H. L. *Organometallics* **1997**, *16*, 1241–1246. (e) Trimmel, G.; Slugovc, C.; Wiede, P.; Mereiter, K.; Sapunov, V. N.; Schmid, R.; Kirchner, K. *Inorg. Chem.* **1997**, *36*, 1076–1083. (f) Gemel, C.; Kickelbick, G.; Schmid, R.; Kirchner, K. *J. Chem. Soc., Dalton Trans.* **1997**, 2113–2117. (g) Slugovc, C.; Doberer, D.; Gemel, C.; Schmid, R.; Kirchner, K.; Winkler, B.; Stelzer, F. *Monatsh. Chem.* **1998**, *129*, 221–233. (h) Slugovc, C.; Mauthner, K.; Kacetl, M.; Mereiter, K.; Schmid, R.; Kirchner, K. *Chem.−Eur. J.* **1998**, *4*, 2043–2050. (i) Slugovc, C.; Mereiter, K.; Schmid, R.; Kirchner, K. *J. Am. Chem. Soc.* **1998**, *120*, 6175–6176. (j) Slugovc, C.; Schmid, R.; Kirchner, K. *Coord. Chem. Rev.* **1999**, *185−186*, 109–126. (k) Cadierno, V.; Díez, J.; Pilar Gamasa, M.; Gimeno, J.; Lastra, E. *Coord. Chem. Rev.* **1999**, *193−195*, 147–205. (l) Lo, Y.-H.; Lin, Y.-C.; Lee, G.-H.; Wang, Y. *Organometallics* **1999**, *18*, 982–988. (m) Buriez, B.; Burns, I. D.; Hill, A. F.; White, A. J. P.; Williams, D. J.; Wilton-Ely, J. D. E. T. *Organometallics* **1999**, *18*, 1504–1516. (n) Slugovc, C.; Gemel, C.; Shen, J.-Y.; Doberer, D.; Schmid, R.; Kirchner, K.; Mereiter, K. *Monatsh. Chem.* **1999**, *130*, 363–375. (o) Slugovc, C.; Mereiter, K.; Schmid, R.; Kirchner, K. *Eur. J. Inorg. Chem.* **1999**, 1141–1149. (p) Pavlik, S.; Gemel, C.; Slugovc, C.; Mereiter, K.; Schmid, R.; Kirchner, K. *J. Organomet. Chem.* **2001**, *617−618*, 301–310.

(2) Otero, A.; Fernández-Baeza, J.; Tejeda, J.; Antiñolo, A.; Carrillo-Hermosilla, F.; Díez-Barra, E.; Lara-Sánchez, A.; Fernández-López, M.; Lanfranchi, M.; Pellinghelli, M. A. *J. Chem. Soc., Dalton Trans.* **1999**, 3537–3539.

(3) (a) Otero, A.; Fernández-Baeza, J.; Tejeda, J.; Antiñolo, A.; Carrillo-Hermosilla, F.; Díez-Barra, E.; Lara-Sánchez, A.; Fernández-López, M. *J. Chem. Soc., Dalton Trans.* **2000**, 2367–2374. (b) Otero, A.; Fernández-Baeza, J.; Antiñolo, A.; Carillo-Hermosilla, F.; Tejeda, J.; Díez-Barra, E.; Lara-Sanchez, A.; Sanchez-Barba, L.; López-Solera, I. *Organometallics* **2001**, *20*, 2428–2430. (c) Beck, A.; Weibert, B.; Burzlaff, N. *Eur. J. Inorg. Chem.* **2001**, 521–527. (d) Burzlaff, N.; Hegelmann, I. *Inorg. Chim. Acta* **2002**, *329*, 147–150. (e) Otero, A.; Fernández-Baeza, J.; Antiñolo, A.; Carillo-Hermosilla, F.; Tejeda, J.; Lara-Sanchez, A.; Sanchez-Barba, L.; Fernández-López, M.; Rodríguez, A. M.; López-Solera, I. *Inorg. Chem.* **2002**, *41*, 5193–5202. (f) Hegelmann, I.; Beck, A.; Eichhorn, C.; Weibert, B.; Burzlaff, N. *Eur. J. Inorg. Chem.* **2003**, 339–347. (g) Beck, A.; Barth, A.; Hübner, E.; Burzlaff, N. *Inorg. Chem.* **2003**, *42*, 7182–7188. (h) Otero, A.; Fernández-Baeza, J.; Antiñolo, A.; Tejeda, J.; Lara-Sanchez, A.; Sanchez-Barba, L.; Rodríguez, A. M. *Eur. J. Inorg. Chem.* **2004**, 260–266. (i) Otero, A.; Fernández-Baeza, J.; Antiñolo, A.; Tejeda, J.; Lara-Sanchez, A.; Sanchez-Barba, L.; Fernández-López, M.; López-Solera, I. *Inorg. Chem.* **2004**, *43*, 1350–1358. (j) Otero, A.; Fernández-Baeza, J.; Antiñolo, A.; Tejeda, J.; Lara-Sánchez, A. *J. Chem. Soc., Dalton Trans.* **2004**, 1499–1510.

(4) Burzlaff, N.; Hegelmann, I.; Weibert, B. *J. Organomet. Chem.* **2001**, *626*, 16–23.

(5) López-Hernández, A.; Müller, R.; Kopf, H.; Burzlaff, N. *Eur. J. Inorg. Chem.* **2002**, 671–677.

10.1021/om8006129 CCC: $40.75 © 2008 American Chemical Society
Publication on Web 10/25/2008

$(CH_2CH_2PPh_2)_2$) or Cp have been investigated according to their reactivity. For example, ruthenium vinylidene and allenylidene complexes do add water, alcohols, or even acetone to the cumulenylidene moiety.[11−13] Although in many cases the addition of alcohols to the cumulenylidene complexes results in alkoxycarbene complexes,[8,14−19] there are other examples where no reaction with water or alcohols was achieved.[10,20]

Furthermore, there are also several examples for the addition of amines to vinylidene and allenylidene ruthenium complexes.[11,18,21−26] In the resulting aminocarbene complexes the resonance structure with the double bond between the α carbon and the nitrogen atom (**II** in Figure 1) is the most important according to X-ray structure analyses.[25]

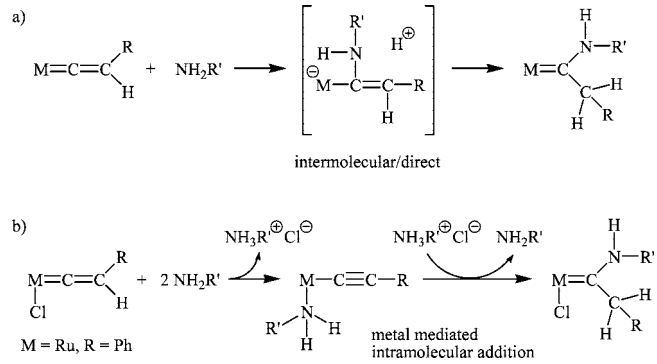

Figure 2. Possible mechanisms for the amine addition to vinylidene ligands.

Nevertheless, there are only a few examples so far in which amines add to the α carbon atom of ruthenium allenylidene complexes.[18,21,25,26] In addition to this rather diverse reactivity of ruthenium cumulenylidene complexes, the mechanism for the reaction of amines with vinylidene complexes is quite controversial. In contrast to the commonly adopted intermolecular and direct mechanism,[27] (Figure 2a) Bianchini et al. suggested a metal-mediated intramolecular mechanism.[23] They report that 2 equiv of amine are necessary for the completion of the reaction in the case of $[RuCl_2(=C=CHPh)(PNP)]$.[11,22−24] Thus, they deduce that in the first step one chlorido ligand is substituted by an amine molecule. After that, an intramolecular addition of the coordinated amine to the carbene ligand takes place (Figure 2b). In contrast, Pavlik et al. observed an intramolecular addition of the amine functionality of the PPh_2NH^nPr ligand for $[Ru(\eta^5\text{-}C_5H_5)(=C=CPh_2)(PPh_2NH^nPr)_2][CF_3SO_3]$.[21] In this case it is almost impossible for the nitrogen atom to have any contact with the metal center. So there are probably different routes for the addition of amines to form ruthenium aminocarbene complexes from vinylidene complexes.

Finally, inspired by the metathesis reaction and Grubbs' catalysts,[28−31] recently neutral and cationic ruthenium Tp carbene complexes have been reported that still show some activity in ring-closing metathesis (RCM).[7] This aroused our interest to investigate further the synthesis and reactivity of ruthenium aminocarbene and ruthenium benzylidene complexes bearing the bpza and bdmpza ligand.

Thus, here we report on the reaction of ruthenium bdmpza cumulenylidene complexes with amines yielding neutral aminocarbene complexes and on ruthenium bpza and bdmpza

(6) (a) Bruce, M. I. *Chem. Rev.* **1991**, *91*, 197–257. (b) Tenorio, M. A. J.; Tenorio, M. J.; Puerta, M. C.; Valerga, P. *Organometallics* **1997**, *16*, 5528–5535. (c) Slugovc, C.; Sapunov, V. N.; Wiede, P.; Mereiter, K.; Schmid, R.; Kirchner, K. *J. Chem. Soc., Dalton Trans.* **1997**, 4209–4216. (d) Bruce, M. I. *Chem. Rev.* **1998**, *98*, 2797–2858. (e) Slugovc, C.; Mereiter, K.; Schmid, R.; Kirchner, K. *Organometallics* **1998**, *17*, 827–831. (f) Slugovc, C.; Mauthner, K.; Kacetl, M.; Mereiter, K.; Schmid, R.; Kirchner, K. *Chem.−Eur. J.* **1998**, *4*, 2043–2050. (g) Jiménez-Tenorio, M. A.; Jiménez-Tenorio, M.; Puerta, M. C.; Valerga, P. *Organometallics* **2000**, *19*, 1333–1342. (h) Rigaut, S.; Touchard, D.; Dixneuf, P. H. *Coord. Chem. Rev.* **2004**, *248*, 1585–1601. (i) Pavlik, S.; Schmid, R.; Kirchner, K.; Mereiter, K. *Monatsh. Chem.* **2004**, *135*, 1349–1357. (j) Pavlik, S.; Mereiter, K.; Puchberger, M.; Kirchner, K. *J. Organomet. Chem.* **2005**, *690*, 5497–5507.

(7) Sanford, M. S.; Henling, L. M.; Grubbs, R. H. *Organometallics* **1998**, *17*, 5384–5389.

(8) Rüba, E.; Gemel, C.; Slugovc, C.; Mereiter, K.; Schmid, R.; Kirchner, K. *Organometallics* **1999**, *18*, 2275–2280.

(9) Sanford, M. S.; Valdez, M. R.; Grubbs, R. H. *Organometallics* **2001**, *20*, 5455–5463.

(10) Kopf, H.; Pietraszuk, C.; Hübner, E.; Burzlaff, N. *Organometallics* **2006**, *25*, 2533–2546.

(11) Bianchini, C.; Casares, J. A.; Peruzzini, M.; Romerosa, A.; Zanobini, F. *J. Am. Chem. Soc.* **1996**, *118*, 4585–4594.

(12) Esteruelas, M. A.; Gómez, A. V.; Lahoz, F. J.; López, A. M.; Oñate, E.; Oro, L. A. *Organometallics* **1996**, *15*, 3423–3435.

(13) Esteruelas, M. A.; Gómez, A. V.; López, A. M.; Modrego, J.; Oñate, E. *Organometallics* **1997**, *16*, 5826–5835.

(14) (a) Bruce, M. I.; Swincer, A. G.; Wallis, R. C. *J. Organomet. Chem.* **1979**, *171*, C5−C8. (b) Consiglio, G.; Morandini, F.; Ciani, G. F.; Sironi, A. *Organometallics* **1986**, *5*, 1976–1983. (c) Bruce, M. I.; Cifuentes, M. P.; Snow, M. R.; Tiekink, E. R. T. *J. Organomet. Chem.* **1989**, *359*, 379–399. (d) Nombel, P.; Lugan, N.; Mathieu, R. *J. Organomet. Chem.* **1995**, *503*, C22−C25.

(15) (a) Gamasa, M. P.; Gimeno, J.; González-Bernardo, C.; Borge, J.; García-Granda, S. *Organometallics* **1997**, *16*, 2483–2485. (b) Esteruelas, M. A.; Gómez, A. V.; López, A. M.; Oñate, E.; Ruiz, N. *Organometallics* **1998**, *17*, 2297–2306.

(16) Bonomo, L.; Stern, C.; Solari, E.; Scopelliti, R.; Floriani, C. *Angew. Chem.* **2001**, *113*, 1497–1500.

(17) González-Herrero, P.; Weberndörfer, B.; Ilg, K.; Wolf, J.; Werner, H. *Organometallics* **2001**, *20*, 3672–3685.

(18) (a) Buil, M. L.; Esteruelas, M. A.; López, A. M.; Oñate, E. *Organometallics* **2003**, *22*, 162–171. (b) Buil, M. L.; Esteruelas, M. A.; López, A. M.; Oñate, E. *Organometallics* **2003**, *22*, 5274–5284.

(19) (a) Ouzzine, K.; Le Bozec, H.; Dixneuf, P. H. *J. Organomet. Chem.* **1986**, *317*, C25−C27. (b) Le Bozec, H.; Ouzzine, K.; Dixneuf, P. H. *Organometallics* **1991**, *10*, 2768–2772. (c) Cadierno, V.; Pilar Gamasa, M.; Gimeno, J.; Iglesias, L. *Inorg. Chem.* **1999**, *38*, 2874–2879.

(20) (a) Wolinska, A.; Touchard, D.; Dixneuf, P. H. *J. Organomet. Chem.* **1991**, *420*, 217–226. (b) Pirio, N.; Touchard, D.; Toupet, L.; Dixneuf, P. H. *J. Chem. Soc., Chem. Commun.* **1991**, 980–982. (c) Touchard, D.; Pirio, N.; Dixneuf, P. H. *Organometallics* **1995**, *14*, 4920–4928. (d) Cadierno, V.; Pilar Gamasa, M.; Gimeno, J.; González-Cueva, M.; Lastra, E.; Borge, J.; García-Granda, S.; Pérez-Carreño, E. *Organometallics* **1996**, *15*, 2137–2147. (e) Cadierno, V.; Pilar Gamasa, M.; Gimeno, J.; López-González, M. C.; Borge, J.; García-Granda, S. *Organometallics* **1997**, *16*, 4453–4463. (f) Crochet, P.; Demerseman, B.; Vallejo, M. I. *Organometallics* **1997**, *16*, 5406–5415.

(21) Pavlik, S.; Mereiter, K.; Puchberger, M.; Kirchner, K. *Organometallics* **2005**, *24*, 3561–3575.

(22) (a) Bianchini, C.; Peruzzini, M.; Romerosa, A.; Zanobini, F. *Organometallics* **1995**, *14*, 3152–3152. (b) Bianchini, C.; Purches, G.; Zanobini, F.; Peruzzini, M. *Inorg. Chim. Acta* **1998**, *272*, 1–3.

(23) Bianchini, C.; Masi, D.; Romerosa, A.; Zanobini, F.; Peruzzini, M. *Organometallics* **1999**, *18*, 2376–2386.

(24) Fillaut, J.-L.; De los Rios, I.; Masi, D.; Romerosa, A.; Zanobini, F.; Peruzzini, M. *Eur. J. Inorg. Chem.* **2002**, 935–942.

(25) Bernad, D. J.; Esteruelas, M. A.; López, A. M.; Modrego, J.; Puerta, M. C.; Valerga, P. *Organometallics* **1999**, *18*, 4995–5003.

(26) Jiménez-Tenorio, M.; Palacios, M. D.; Puerta, M. C.; Valerga, P. *J. Organomet. Chem.* **2004**, *689*, 2776–2785.

(27) (a) Boland-Lussier, B. E.; Hughes, R. P. *Organometallics* **1982**, *1*, 635–639. (b) Kostić, N. M.; Fenske, R. F. *Organometallics* **1982**, *1*, 974–982. (c) Blackburn, B. K.; Davies, S. G.; Sutton, K. H.; Whittaker, M. *Chem. Soc. Rev.* **1988**, *17*, 147–179. (d) Delbecq, F. *J. Organomet. Chem.* **1991**, *406*, 171–182. (e) Pilar Gamasa, M.; Gimeno, J.; Lastra, E.; Lanfranchi, M.; Tiripicchio, A. *J. Organomet. Chem.* **1992**, *430*, C39−C43.

(28) Schwab, P.; Grubbs, R. H.; Ziller, J. W. *J. Am. Chem. Soc.* **1996**, *118*, 100–110.

(29) (a) Scholl, M.; Ding, S.; Lee, C. W.; Grubbs, R. H. *Org. Lett.* **1999**, *1*, 953–956. (b) Scholl, M.; Trnka, T. M.; Morgan, J. P.; Grubbs, R. H. *Tetrahedron Lett.* **1999**, *40*, 2247–2250. (c) Weskamp, T.; Kohl, F. J.; Hieringer, W.; Gleich, D.; Herrmann, W. A. *Angew. Chem.* **1999**, *111*, 2573–2576. (d) Huang, J.; Stevens, E. D.; Nolan, S. P.; Petersen, J. L. *J. Am. Chem. Soc.* **1999**, *121*, 2674–2678. (e) Morgan, J. P.; Grubbs, R. H. *Org. Lett.* **2000**, *2*, 3153–3155.

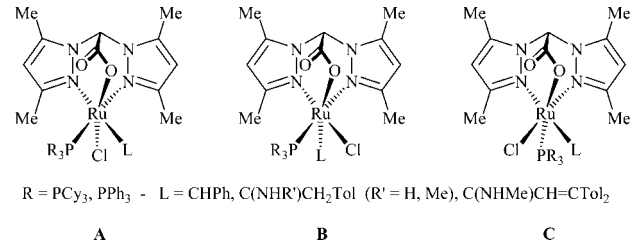

Figure 3. The three different structural isomers.

benzylidene complexes, which are active in the RCM of diethyl diallylmalonate.

Results and Discussion

(A) Isomers of bpza Class Complexes. In our recent report on ruthenium cumulenylidene complexes we observed various structural isomers for the bdmpza cumulenylidene complexes.[10] Also for the carbene complexes discussed in this report three different structural isomers are conceivable, which are (A) chlorido ligand *trans* to carboxylate, (B) carbene ligand *trans* to carboxylate, and (C) phosphine ligand *trans* to carboxylate (Figure 3).

Due to the *trans* influence of the pyrazole acceptor ligands, coordination of the phosphine donor *trans* to the carboxylate is very unlikely. Furthermore, all the NOE experiments we performed for the carbene complexes, which will be discussed later in detail, showed cross-peaks between the phosphine ligand signals and the signals of only one pyrazole donor. Therefore, the formation of isomer **C** can be excluded, so far. Both isomers **A** and **B** are racemic mixtures of two enantiomers. Because of loss of the C_s symmetry in these isomers, two different sets of NMR signals are expected for the two pyrazolyl groups. For isomers of type **A** and **B** the pyrazole group next to the remaining phosphine ligand will be marked by a prime (e.g., $Me^{3'}$) throughout this text.

(B) Syntheses of Aminocarbene Complexes Starting from Cumulenylidene Ligands. So far we observed no reaction of the vinylidene complexes [Ru(bdmpza)Cl(=C=CHPh)(PPh_3)] and [Ru(bdmpza)Cl(=C=CHTol)(PPh_3)] (**1**) with water.[10] A reaction mixture of **1** in refluxing methanol showed only unreacted vinylidene complex after 14 h. A similar stability to water and methanol is apparent for the allenylidene complexes [Ru(bdmpza)Cl(=C=C=CPh_2)(PPh_3)] and [Ru(bdmpza)Cl(=C=C=$CTol_2$)(PPh_3)] (**2a**, **2b**) [**2a**: isomer **A**, allenylidene *trans* to pyrazole; **2b**: isomer **B**, allenylidene *trans* to carboxylate] since nondried methanol can be used in the purification of these complexes via column chromatography.[10] Therefore, our studies first focused on the reactivity of **1** toward NH_3, NH_2Me, and $NHMe_2$. Former DFT calculations already showed a rather small energy difference between the type A and type B isomers in the case of the allenylidene complexes.[10]

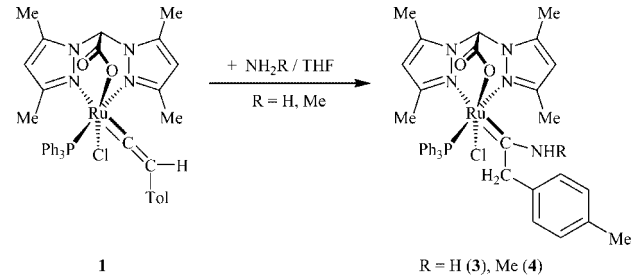

Figure 4. Reaction of ammonia and amines with the vinylidene complex **1** yielding the carbene complexes **3** and **4**.

For the reaction with ammonia, gaseous NH_3 was passed through a suspension of **1** in THF. Although after less than 1 min the orange suspension changed to a yellow solution, for completion of the reaction the mixture had to be stirred for an additional 15 min under an atmosphere of NH_3 (Figure 4). It is noteworthy that according to Bianchini et al.[23] the reaction of NH_3 with *fac,cis*-[$RuCl_2$(=C=CHPh)(PNP)] took much longer to complete. The most significant change in the ^{1}H NMR spectrum of [Ru(bdmpza)Cl(=C(NH_2)CH_2Tol)(PPh_3)] (**3**) is observed for the H_β signal, which changes from one doublet at 4.89 ppm ($^4J_{HP}$ = 4.9 Hz)[10] to an AB system with doublet signals at 3.86 and 4.21 ppm (J_{AB} = 19.2 Hz). This AB system is caused by the chirality of the C_1 symmetric complex.

Two broader doublets at 8.05 and 8.74 ppm ($^2J_{HH}$ = 3.6 Hz) have been assigned to the NH_2 functionality. In the ^{13}C NMR spectrum the C_α of the product [Ru(bdmpza)Cl(=C(NH_2)-CH_2Tol)(PPh_3)] (**3**) is found as a doublet at 271.2 ppm ($^2J_{CP}$ = 14.6 Hz). This is a remarkable high-field shift compared to the C_α ^{13}C NMR signal of the vinylidene complex **1** at 364.2 ppm. The C_β signal of complex **3** is observed at 53.0 ppm. The values agree well with those reported by Bianchini et al. for the complex *fac,cis*-[$RuCl_2$(=C(NH_2)CH_2Ph)(PNP)] [^{1}H NMR: 4.65 ppm (H_β), 8.34 and 10.14 ppm (broad, NH_2); ^{13}C NMR: 58.7 ppm (C_β), 261.6 ppm ($^2J_{CP}$ = 11.4 Hz, C_α)].[23] The ^{31}P NMR signal of complex **3** is found at 50.4 ppm and thus significantly different from that of the vinylidene complex precursor **1** (37.5 ppm).

In an analogous reaction a 2-fold excess of a methylamine solution (0.1 M in THF) was added to a suspension of the vinylidene complex [Ru(bdmpza)Cl(=C=CHTol)(PPh_3)] (**1**) in THF. Again, the orange suspension changed to a yellow solution within a minute. After 15 min the reaction was complete according to the NMR data (Figure 4). The ^{1}H NMR spectrum of the formed complex [Ru(bdmpza)Cl(=C(NHMe)CH_2Tol)-(PPh_3)] (**4**) exhibits an AB system for the CH_2 group at 3.29 and 4.00 ppm (J_{AB} = 12.4 Hz). A doublet at 3.16 ppm ($^3J_{HH}$ = 3.6 Hz) and a smooth resonance at 9.84 ppm can be assigned to the NHMe group. The ^{13}C NMR spectrum resembles that of complex **3**. The C_α signal is found at 265.1 ppm ($^2J_{CP}$ = 15.3 Hz), and the C_β shows a resonance at 43.9 ppm. Additionally, there is a singlet signal at 35.6 ppm, which is assigned to the NMe group. The ^{31}P NMR spectrum shows a signal at 47.0 ppm. This value is close to that of the aminocarbene complex **3** (50.4 ppm).

Crystals suitable for X-ray diffraction experiments were obtained from a CH_2Cl_2 solution of **4** layered with *n*-hexane. The data confirm the molecular structure deduced by two-dimensional NMR analyses and agrees well with that of other bdmpza ruthenium carbene complexes, which we reported on

(30) (a) Nguyen, S. T.; Johnson, L. K.; Grubbs, R. H. *J. Am. Chem. Soc.* **1992**, *114*, 3974–3975. (b) Nguyen, S. T.; Grubbs, R. H. *J. Am. Chem. Soc.* **1993**, *115*, 9858–9859. (c) Tallarico, J. A.; Bonitatebus, P. J., Jr.; Snapper, M. L. *J. Am. Chem. Soc.* **1997**, *119*, 7157–5158. (d) Ulman, M.; Grubbs, R. H. *Organometallics* **1998**, *17*, 2484–2489. (e) Hinderling, C.; Adlhart, C.; Chen, P. *Angew. Chem.* **1998**, *110*, 2831–2835. (f) Cucullu, M. E.; Li, C.; Nolan, S. P. *Organometallics* **1998**, *17*, 5565–5568. (g) Aagaard, O. M.; Meier, R. J.; Buda, F. *J. Am. Chem. Soc.* **1998**, *120*, 7174–7182. (h) Adlhart, C.; Hinderling, C.; Baumann, H.; Chen, P. *J. Am. Chem. Soc.* **2000**, *112*, 8204–8214. (i) Trnka, T. M.; Grubbs, R. H. *Acc. Chem. Res.* **2001**, *34*, 18–29. (j) Vyboishchikov, S. F.; Bühl, M.; Thiel, W. *Chem.—Eur. J.* **2002**, *8*, 3962–3975. (k) Adlhart, C.; Chen, P. *Angew. Chem.* **2002**, *114*, 4668–4671. (l) Adlhart, C.; Chen, P. *J. Am. Chem. Soc.* **2004**, *126*, 3496–3510. (m) Costabile, C.; Cavallo, L. *J. Am. Chem. Soc.* **2004**, *126*, 9592–9600. (n) Straub, B. F. *Angew. Chem.* **2005**, *117*, 6129–6132. (o) Lippstreu, J. J.; Straub, B. F. *J. Am. Chem. Soc.* **2005**, *127*, 7444–7457. (p) Deshmukh, P. H.; Blechert, S. *Dalton Trans.* **2007**, 2479–2491.

(31) Fürstner, A. *Angew. Chem.* **2000**, *112*, 3140–3172.

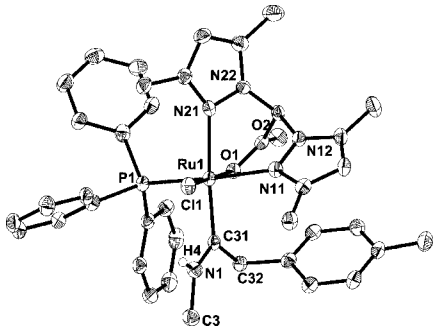

Figure 5. Molecular structure of [Ru(bdmpza)Cl(=C(NHMe)-CH_2Tol)(PPh_3)] (**4**). Thermal ellipsoids are drawn at the 50% probability level. Hydrogen atoms and solvent molecules are omitted for clarity. Only one of the two molecules in the asymmetric unit is depicted.

Table 1. Selected Bond Lengths (Å) and Angles (deg) of the Two Aminocarbene Complexes 4

Ru−O1	2.094(2)	2.104(2)	O1−Ru−C31	89.88(12)	89.04(12)
Ru−N21	2.173(3)	2.211(3)	O1−Ru−Cl	174.33(6)	176.79(6)
Ru−C31	1.988(3)	1.982(3)	O1−Ru−N11	84.84(10)	86.13(10)
Ru−Cl	2.4424(9)	2.4329(9)	N21−Ru−C31	174.95(12)	173.96(12)
Ru−P	2.3149(9)	2.3201(9)	N21−Ru−P	95.22(7)	95.26(7)
Ru−N11	2.163(3)	2.131(3)	N21−Ru−N11	81.69(10)	79.86(10)
C31−N1	1.321(4)	1.323(4)	C31−Ru−Cl	91.04(10)	90.36(10)
N1−C3	1.480(5)	1.463(5)	C31−Ru−P	87.49(9)	90.23(10)
			C31−Ru−N11	94.89(12)	94.31(12)
			Ru−C31−N1	122.5(2)	122.2(3)
			Ru−C31−C32	122.2(2)	122.3(2)
N1−C31−N21−N22	157.5(3)	166.4(3)	N1−C31−C32	115.3(3)	115.6(3)

recently.[10] Two molecules of **4** are found in the asymmetric unit. The molecular structure of one of these molecules is depicted in Figure 5. Selected bond distances, angles, and torsion angles are listed in Table 1.

The two molecules of **4** in the asymmetric unit are identical, except one interesting feature. The aminocarbene moieties are almost coplanar to the pyrazole donor in *trans* position. This is indicated by the torsion angles ∠N1−C31−N21−N22 (157.5(3)° and 166.4(3)°). Obviously these torsion angles differ by 8.9°. On the other hand the Ru−N distances *trans* to the aminocarbene ligand differ slightly in the two molecular structures of complex **4** (2.173(3) and 2.211(3) Å). This is caused by the *trans* influence of the π-accepting Fischer carbene ligand. Thus, the better the coplanarity between the aminocarbene ligand and the *trans* pyrazole donor, the longer the observed Ru−N distance.

The distances d(Ru−C_α) of complex **4** [1.988(3) and 1.982(3) Å] lie exactly in the range usually observed for neutral ruthenium aminocarbene complexes such as (*S*)-(−)-*fac,cis*-[$RuCl_2$(=C(NH(CHMe(1-naphthyl)))CH_2Ph)(PNP)] [d(Ru−C_α) = 1.99(2) Å][25] or [RuCp(=C(NHPh)CH_2Ph)(κ^1*P*-PPh_2O)(PPh_2NHPh)] [d(Ru−C_α) = 1.984(12) Å].[21] Also the distance reported for the cationic complex [RuTp(κ^2(*C,P*)=C(N^{n}PrPPh_2)-$CH_2C_6H_4$Me)(κ^1*P*-PPh_2NH^{n}Pr)][CF_3SO_3] [d(Ru−C_α) = 1.993(1) Å] is close to these values. The bond distances d(C_α−N) in [Ru(bdmpza)Cl(=C(NHMe)CH_2Tol)(PPh_3)] (**4**) are 1.321(4) and 1.323(4) Å, characteristic for Fischer-type aminocarbene complexes.

For the complex *fac,cis*-[$RuCl_2$(=C=CHPh)(PNP)] Bianchini et al. reported a fast color change from orange to yellow with primary amines and no reaction with secondary alkylamines.[23] They suggested a mechanism with two amine molecules involved, proceeding through an alkynyl complex in which one chlorido ligand is exchanged by a coordinated primary amine.

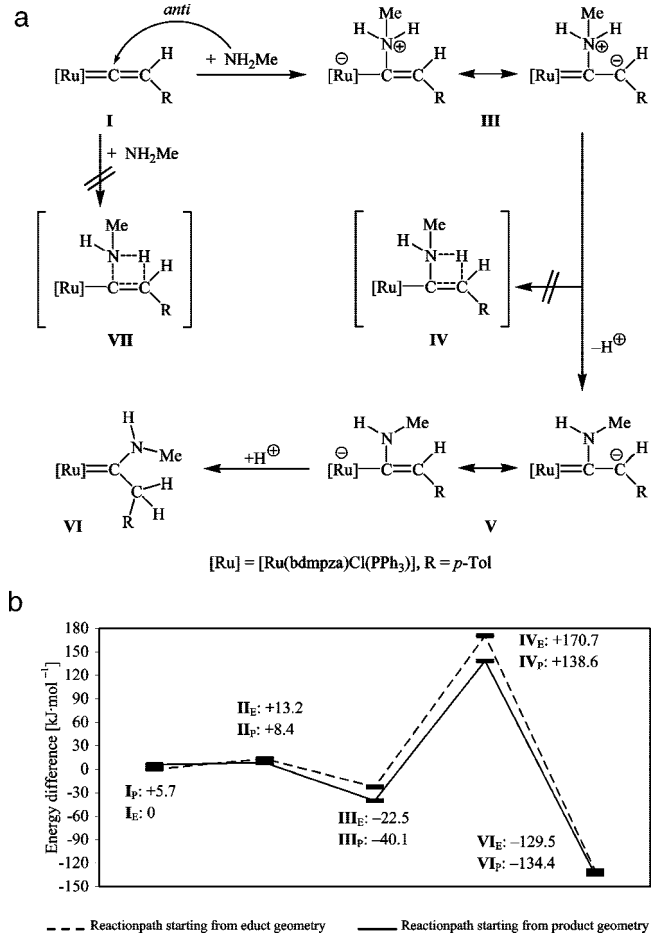

Figure 6. (a) Reaction scheme of the addition of NH_2Me to **1** yielding **4**. (b) Energy scheme of the addition of NH_2Me to **1** yielding **4**.

Secondary and tertiary amines did not coordinate to the ruthenium center, and the formation of the aminocarbene complexes failed in these cases.

Thus we decided to study also the reaction of [Ru(bdmpza)-Cl(=C=CHTol)(PPh_3)] (**1**) with dimethylamine. Similar to the findings of Bianchini et al. no color change occurred after 15 h at ambient temperature even with a 10-fold excess of dimethylamine (0.1 M in THF). NMR spectra of the reaction mixture still showed the vinylidene complex **1**.

In order to investigate whether the reaction of NH_2Me with [Ru(bdmpza)Cl(=C=CHTol)(PPh_3)] (**1**) takes place via an intermolecular mechanism with direct nucleophilic attack at C_α or via Bianchini's intramolecular mechanism with alkynyl complex and coordinated NH_2Me, we repeated the reaction of **1** with only 0.8 equiv of NH_2Me instead of a 2-fold excess. To avoid higher concentrations, the amine solution was added very slowly over a period of 30 min, during which time the reaction took place. NMR spectra of the reaction mixture showed traces of **1** and the aminocarbene complex **4**, but no other intermediate complex. There was also no IR absorption at 2055 cm^{-1}, indicating a C≡C triple bond, as observed by Bianchini.[23] Thus, we assume that an intramolecular mechanism via an alkynyl complex can be excluded in our case.

To support the intermolecular direct mechanism, additional DFT calculations (LACVP*/BP86) regarding this reaction pathway (Figure 6a) were performed. Since the lowest conformers of the product **4** (Figure 7j) and the educt **1** (Figure 7a) differ in rotation around the Ru−C bond, both reaction pathways

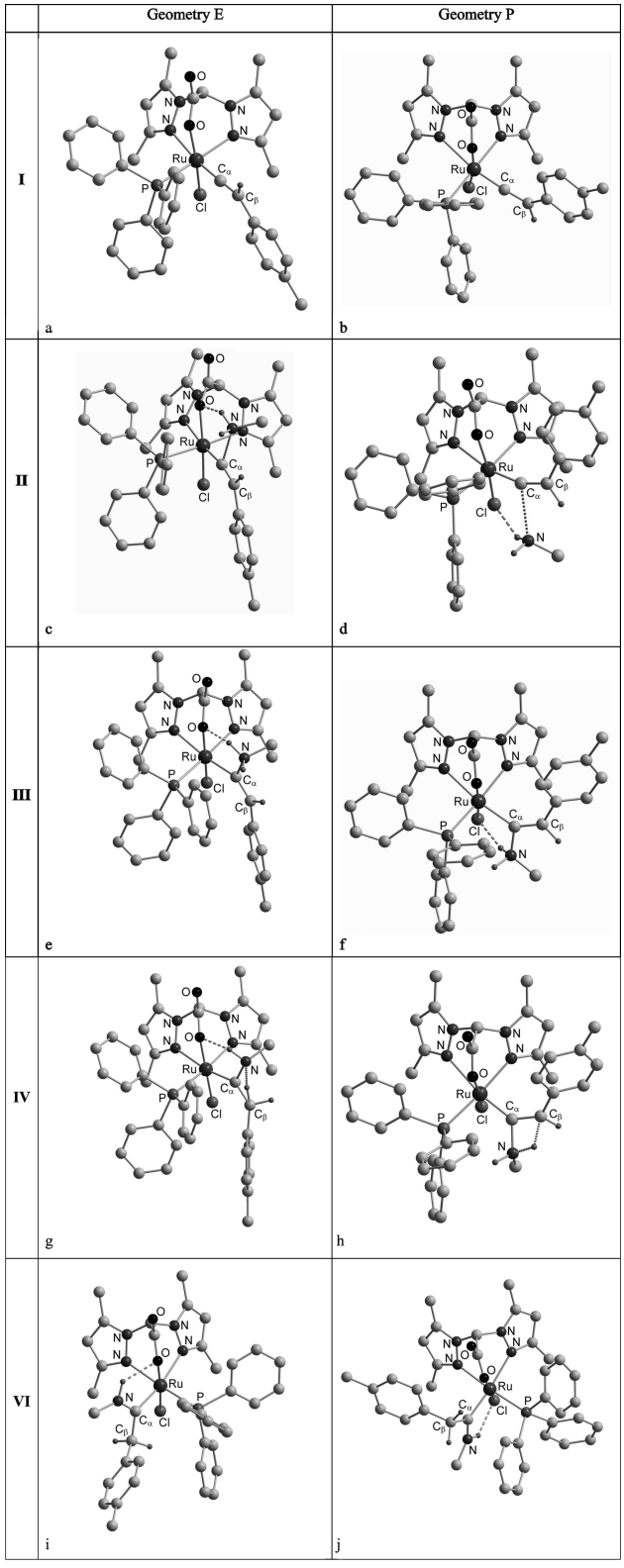

Figure 7. Structures resulting from the DFT calculations: (a) $\mathbf{I_E}$, the lowest energy conformer of **1**; (b) $\mathbf{I_P}$, the second conformer of **1** achieved after rotation around the Ru−C bond; (c) $\mathbf{II_E}$, the transition state of the addition of methylamine to $\mathbf{I_E}$; (d) $\mathbf{II_P}$, the transition state of the addition of methylamine to $\mathbf{I_P}$; (e) $\mathbf{III_E}$, the stable intermediate of $\mathbf{I_E}$ with methylamine; (f) $\mathbf{III_P}$, the stable intermediate of $\mathbf{I_P}$ with methylamine; (g) $\mathbf{IV_E}$, the transition state of the tautomerization from $\mathbf{III_E}$ to $\mathbf{VI_E}$; (h) $\mathbf{IV_P}$, the transition state of the tautomerization from $\mathbf{III_P}$ to $\mathbf{VI_P}$; (i) $\mathbf{VI_E}$, the unfavorable rotational conformer of the product **4**; and (j) $\mathbf{VI_P}$, the product **4** of the reaction.

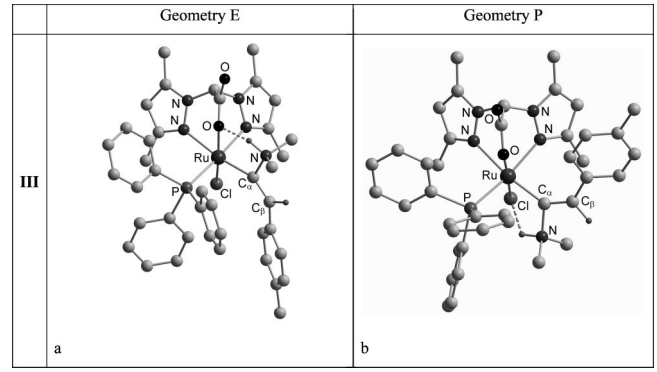

Figure 8. Structures resulting from the DFT calculations: (a) $\mathbf{III_E}$, the stable intermediate of $\mathbf{I_E}$ with dimethylamine, and (b) $\mathbf{III_P}$, the stable intermediate of $\mathbf{I_P}$ with dimethylamine.

starting with educt (E) or product (P) geometry were calculated. As we reported recently,[10] this rotational barrier between $\mathbf{I_E}$ and $\mathbf{I_P}$ is low enough to expect free rotation at room temperature. In a first result (Figure 6b), a stable intermediate (**III**) was found in the case of the direct addition of the amine to C_α of the vinylidene ligand (**I**). The low (<9 kJ/mol) transition state $\mathbf{II_P}$ (Figure 7c and d) towards this intermediate (Figure 7e and f) and relatively high yield of energy (>40 kJ/mol) upon formation of the intermediate $\mathbf{III_P}$ make this two-step reaction pathway more favorable than a concerted reaction (**VII**). Furthermore, tautomerization from **III** to **VI** via intramolecular H-shift resulted in a high transition state $\mathbf{IV_P}$ (>138 kJ/mol). Hence, at room temperature a reaction via an intermolecular stepwise mechanism (**V**) has to be assumed.

The geometry-optimized structures of the DFT calculations revealed an interesting hydrogen bridge between one of the hydrogen atoms of the methylamine residue and either the carboxylato or the chlorido ligand in the intermediates $\mathbf{III_E}$ and $\mathbf{III_P}$ (Figure 7e and f). Breaking of this hydrogen bridge during the hypothetical intramolecular hydrogen shift in $\mathbf{IV_E}$ and $\mathbf{IV_P}$ might be one reason for the high transition state (Figure 7g and h).

Further DFT calculations of the analogous reaction with the secondary amine $NHMe_2$, which does not take place in the laboratory experiment, also exhibit the stable intermediates $\mathbf{III_E}$ and $\mathbf{III_P}$ (analogous to Figure 6b: $\mathbf{III_E}$, +4.1; $\mathbf{III_P}$, −19.5 kJ/mol) with hydrogen bridges between the N−H and the carboxylato or chlorido residue (Figure 8a and b). If one hydrogen atom is fixed in this hydrogen bridge bond, there is, in contrast to the reaction with methylamine, no free hydrogen left, and therefore the productive deprotonation step cannot take place. Instead, in the end the nucleophile will not add but probably dissociate again. Inspired by these observations, the reaction of the vinylidene complex **1** with $NHMe_2$ was repeated (a) in the presence of 0.5 equiv of $[NEt_3H]Cl$ and (b) also with a huge excess thereof. The idea was that $[NEt_3H]Cl$ might be able to protonate the β carbon atom in the intermediate and that this protonation might be followed by a deprotonation of the amino functionality in α position. But no reaction was observed so far. Nevertheless, this could still mean that the final productive deprotonation step is blocked by the formation of the hydrogen bridge, even if protons are available.

DFT calculations regarding MeOH as nucleophile, which were starting from a possible intermediate structure, did not result in a stable intermediate but showed dissociation of methanol instead. This is in accordance with the experimental results, which did not reveal any evidence for reaction products formed by the addition of methanol to **1**.

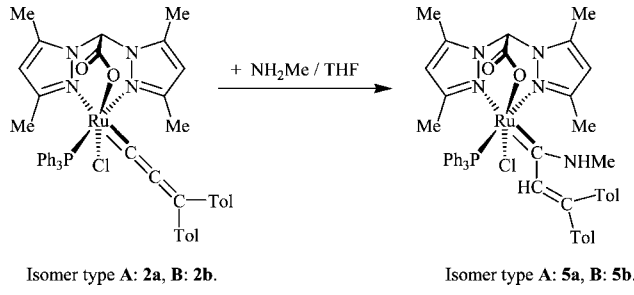

Figure 9. Addition of amines to the allenylidene complexes **2a** and **2b** yielding the carbene complexes **5a** and **5b**.

Generally, the addition of nucleophiles to an allenylidene ligand is possible at the α or γ carbon atom. Thus, we performed DFT calculations for the allenylidene complexes [Ru(bdmpza)Cl(=C=C=CTol$_2$)(PPh$_3$)] (**2a**, **2b**) to determine the orbital coefficients of the LUMOs.[10] In both cases the calculations show a smaller coefficient for the α carbon atom compared to the γ carbon atom. This would mean that weak nucleophiles might attack in γ position, as observed in the case of the chromium complex [Cr(=C=C=C(OMe)NMe$_2$)(CO)$_5$] for the reaction with NH$_3$.[32] But a rearrangement to the α adduct might also occur, as reported for the rhenium complex [Re(=C=C=CPh$_2$)(CO)$_2$(triphos)][OTf] after γ addition of ammonia.[33]

Reaction of the allenylidene complex **2b** with a methylamine solution (0.1 M in THF) takes 18 h at ambient temperature, leading to a clean product that can be isolated by precipitation with *n*-hexane from a CH_2Cl_2 solution and that is characterized as [Ru(bdmpza)Cl(=C(NHMe)CH=CTol$_2$)(PPh$_3$)] (**5b**) (carbene *trans* carboxylate) (Figure 9). Whether a γ attack followed by a rearrangement or a direct α attack has taken place was not investigated.

In the NMR spectra of the allenylidene complexes **2a** and **2b** the two tolyl groups of the allenylidene ligand are spectroscopically equivalent due to rotation of the cumulated chain. After addition of a nucleophile to the α carbon the rotation around the Ru−C$_\alpha$ bond seems to be hindered. Furthermore, the tolyl groups are no longer spectroscopically equivalent. Especially in the ^{13}C NMR spectrum, one can notice two sets of signals for the tolyl groups. Furthermore, the former sharp ^{13}C NMR phosphine signals are broad now, and 2D experiments such as gHMQC do partially fail. In the ^{1}H NMR spectrum two signals at 2.22 and 2.29 ppm can be assigned to the two methyl groups of the tolyl substituents. The methylamino group occurs as a doublet ($^3J_{HH}$ = 8.0 Hz). The NH proton signal can be observed at 8.71 ppm and is, as expected, broad. The ^{13}C NMR spectrum exhibits resonances at 20.5, 20.7, and 36.8 ppm, which can be assigned to the two tolyl and the methylamino methyl groups. The ^{13}C NMR signal of the α carbon is found at 252.1 ppm ($^2J_{CP}$ = 10.1 Hz). These values are close to the respective signals of **3** and **4**. All three complexes agree well in the ^{31}P signals (**5b**: 45.3 ppm; **3**: 50.4 ppm; **4**: 47.0 ppm). Finally, the aminocarbene complex **5b** is confirmed by a M$^+$ peak in a mass spectrum (FAB).

In contrast to these findings, the reaction of allenylidene complex isomer **2a** with a 0.1 M solution of methylamine in THF at ambient temperature leads to a brown mixture within a few minutes. When performing the reaction at 0 °C, a dark yellow product is obtained after 10 min. Unfortunately, the NMR spectra of the assumed product complex [Ru(bdmpza)Cl(=C(NHMe)CH=CTol$_2$)(PPh$_3$)] (**5a**) (carbene *trans* pyrazole) have not yet been completely understood. The resonances of the bdmpza and the triphenylphosphine ligand could be assigned as well as those of the two *para*-tolyl residues. But, so far we were not able to assign the relevant signals of H$_\beta$, C$_\beta$, and C$_\gamma$. The C$_\alpha$ signal in the ^{13}C NMR spectrum (255.3 ppm) and the ^{31}P NMR signal (49.6 ppm) are comparable to those of **3** (271.2 and 50.4 ppm), **4** (265.1 and 47.0 ppm), and **5b** (252.1 and 45.3 ppm). An elemental analysis and a M$^+$ − peak (m/z = 895.4) in the FAB mass spectrum confirm the proposed structure as well as the related alkynyl complex. Due to its betaine structure, this alkynyl complex should exhibit a decreased solubility. Since **5a** seems to be more soluble than **5b**, we propose the structure of **5a** as an aminocarbene complex (Figure 9). A reaction of the allenylidene complexes **2a** and **2b** with gaseous NH$_3$ resulted in unidentifiable mixtures of products.

(C) Syntheses of Benzylidene Complexes and Their Catalytic Activity in Metathesis Reactions. Grubbs' metathesis catalysts of the first and second generation as well as modifications thereof are nowadays common reagents in organic syntheses.[28,29] The mechanism based on the interplay of a 16-VE and a 14-VE ruthenium(II) center is well understood.[34] Several practical and theoretical investigations have been reported that focused on ligand effects and orbital considerations regarding this reaction.[30,35] In general, the design motif of the family of Grubbs' catalysts includes two negatively charged chlorido ligands, one neutral but donating phosphine or NHC ligand, the benzylidene ligand, and an additional ligand (typically phosphine) that dissociates, forming a 14-VE intermediate.

Thus, complexes bearing facial binding tridentate ligands such as Tp or the N,N,O heteroscorpionate ligand bdmpza have to comply with the features of the design motif if these complexes are to be reasonably good catalysts. Although a catalytic activity comparable to those of Grubbs' catalyst of first and second generation will not be possible to achieve for such scorpionate ruthenium complexes, they might have other advantages in the future, such as a well-defined stereochemical surrounding or the possibility of grafting on a solid phase. In 1998 Sanford, Henling, and Grubbs reported on a benzylidene complex, [RuCl(Tp)(=CHPh)(PCy$_3$)], and the related cationic species [Ru(Tp)(=CHPh)(PCy$_3$)(L)]$^+$ (L = H$_2$O, pyridine, CH$_3$CN), which are active in RCM.[7] Therefore, we decided to synthesize various ruthenium complexes bearing the bis(pyrazol-1-yl)-acetate (bpza) and the bdmpza ligands and to test them in metathesis reactions.

In analogy with Sanford et al.,[7] who reacted the potassium salt of the Tp ligand with Grubbs' catalyst, we added K[bpza] to [RuCl$_2$(=CHPh)(PCy$_3$)$_2$] (Figure 10). Within 2 h the reaction was complete at ambient temperature, yielding [Ru(bpza)-Cl(=CHPh)(PCy$_3$)] (**6**) as a green complex. The green color of the product agrees well with that of [RuCl(Tp)(=CHPh)(PCy$_3$)] reported by Sanford.[7]

The most significant NMR signals of [Ru(bpza)Cl(=CHPh)-(PCy$_3$)] (**6**) are those of the benzylidene H$_\alpha$ and the C$_\alpha$. While the proton is found as a doublet in the ^{1}H NMR at 20.09 ppm ($^3J_{HP}$ = 8.0 Hz), the carbon atom exhibits a single signal at 328.3 ppm. Similar values but with a C−P coupling have been reported for the complex [RuCl(Tp)(=CHPh)(PCy$_3$)] [^{1}H NMR: 20.01 ppm (H$_\alpha$, $^3J_{HP}$ = 9.51 Hz), ^{13}C NMR: 333.7 ppm (C$_\alpha$,$^2J_{CP}$

(32) Drexler, M.; Haas, T.; Sze-Man, Y.; Beckmann, H.; Weibert, B.; Fischer, H. *J. Organomet. Chem.* **2005**, *690*, 3700–3713.
(33) Mantovani, N.; Marvelli, L.; Rossi, R.; Bertolasi, V.; Bianchini, C.; de los Rios, I.; Peruzzini, M. *Organometallics* **2002**, *21*, 2382–2394.
(34) Hérrison, J.-L.; Chauvin, Y. *Makromol. Chem.* **1970**, *141*, 161–176.
(35) Ritter, T.; Hejl, A.; Wenzel, A. G.; Funk, T. W.; Grubbs, R. H. *Organometallics* **2006**, *25*, 5740–5745.

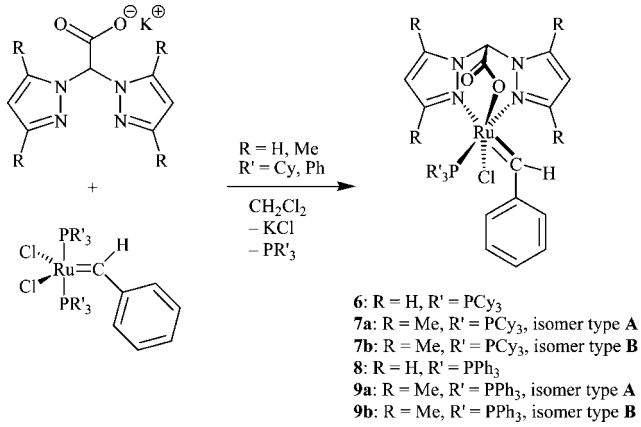

Figure 10. Syntheses of the ruthenium benzylidene complexes **6**−**9b**.

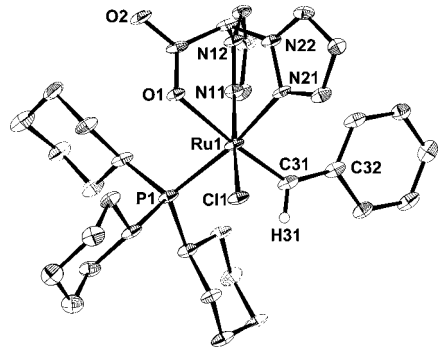

Figure 11. Molecular structure of [Ru(bpza)Cl(=CHPh)(PCy_3)] (**6**) with thermal ellipsoids drawn at the 50% probability level. Most hydrogen atoms and solvent molecules are omitted for clarity.

= 19.3 Hz)].[7] Also none of the C−P couplings are resolved that are observed for some of the pyrazole carbon atoms *trans* to a phosphine ligand.[10]

According to the NMR spectra the formation of only one isomer is observed in the case of the complex [Ru(bpza)-Cl(=CHPh)(PCy_3)] (**6**). This is in contrast to the observations we made for complexes bearing two PPh_3 ligands. Whereas [Ru(bpza)Cl(PPh_3)$_2$], with the sterically less demanding bpza ligand, is a mixture of two isomers, the more bulky bdmpza ligand causes one symmetrical isomer in [Ru(bdmpza)Cl-(PPh_3)$_2$].[5]

On one occasion a single crystalline block of **6** was obtained from a crystallization experiment. An X-ray structure determination revealed a molecular structure of the B isomer type with the benzylidene ligand *trans* to the carboxylate donor for complex **6** (Figure 11), although it cannot be excluded unequivocally that undetected traces of a minor isomer might be the source of the crystals. Furthermore, the result of the X-ray structure analysis is severely affected by disordered dichloromethane solvent molecules. Thus, the molecular structure will not be discussed in detail in this article.

The analogous reaction of [$RuCl_2$(=CHPh)(PCy_3)$_2$] with K[bdmpza] yielded the complex [Ru(bdmpza)Cl(=CHPh)-(PCy_3)] (Figure 10) as a mixture of two green complex isomers **7a** and **7b**, which can be separated by column chromatography. The characteristic ^{1}H NMR α proton signals at 20.47 (**7a**) and 20.45 ppm (**7b**) are split by $^3J_{HP}$ = 11.60 Hz and $^3J_{HP}$ = 8.80 Hz, respectively. The ^{13}C NMR signals of the α carbon atom are observed at 326.4 and 325.7 ppm. In case of complex **7b**, in which the carbene ligand is placed *trans* to the carboxylate donor, a coupling $^2J_{CP}$ was determined to be 15.7 Hz. This value agrees well with the $^2J_{CP}$ = 19.3 Hz coupling reported for [Ru(Tp)Cl(=CHPh)(PCy_3)].[7] Crystals of complex **7b** suitable for X-ray diffraction have been obtained from CH_2Cl_2. The molecular structure confirms the B-type isomer and will be discussed later (Figure 12).

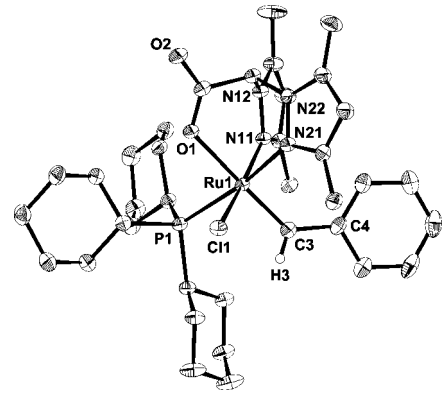

Figure 12. Molecular structure of [Ru(bdmpza)Cl(=CHPh)(PCy_3)] (**7b**) with thermal ellipsoids drawn at the 50% probability level. Most hydrogen atoms and solvent molecules are omitted for clarity.

The result of the X-ray structure analysis of the bpza complex **6** shows a B-type geometry, but this might not represent the major isomer as discussed above. The chemical shift in the ^{31}P NMR spectrum of **6** differs about 6.9 ppm from the bdmpza complex **7b** [δ = 26.6 ppm (**6**) and δ = 19.7 ppm (**7b**)]. On the other hand a similar high-field shift (5.1 ppm) was also observed for the bisphosphine complexes [Ru(bpza)Cl(PPh_3)$_2$] and [Ru(bdmpza)Cl(PPh_3)$_2$].[5] Thus, the ^{31}P NMR signal of **6** agrees well with the type B complex **7b** and indicates that the bpza benzylidene complex **6** mainly forms with geometry type B.

A much cheaper precursor compared to the commercially available Grubbs' catalyst is the benzylidene complex [$RuCl_2$(=CHPh)(PPh_3)$_2$]. Usually, this complex can be converted into the Grubbs' catalyst by replacing PPh_3 by expensive PCy_3.[28] As noted above, in the olefin metathesis reaction catalyzed by complexes with well-coordinated tripodal ligands this phosphine will most likely play the part of a dissociating ligand and thus will be wasted. Therefore, an analogous reaction of [$RuCl_2$(=CHPh)(PPh_3)$_2$][28] with K[bpza] and K[bdmpza] was performed, yielding the ruthenium benzylidene complexes [Ru(bpza)Cl(=CHPh)(PPh_3)] (**8**) and [Ru(bdmpza)Cl(=CHPh)-(PPh_3)] (**9a**, **9b**), respectively (Figure 10). Similar to the bpza complex **6** only one isomer was found in the case of complex **8**. This complex exhibits a ^{1}H NMR signal for the α proton at 18.27 ppm ($^3J_{HP}$ = 12.0 Hz), which agrees well with that of the complexes **6** [20.09 ppm ($^3J_{HP}$ = 8.0 Hz)] and [RuCl(Tp)(=CHPh)(PCy_3)] [20.01 ppm ($^3J_{HP}$ = 9.51 Hz)].[7] The ^{13}C NMR signal of the α carbon atom was observed at 337.8 ppm. This value is also almost identical to those of the complexes **6** (328.3 ppm) and [RuCl(Tp)(=CHPh)-(PCy_3)] (333.7 ppm; $^2J_{CP}$ = 19.3 Hz).[7] In addition to a complete two-dimensional NMR study complex **8** was verified also by a FAB mass spectrum.

As one might expect for a bdmpza complex, we were able to isolate two isomeric complexes [Ru(bdmpza)Cl(=CHPh)-(PPh_3)] (**9a**, **9b**). The most characteristic NMR signals are again those of the α proton and the α carbon atom. For complex **9a**, the isomer with the carbene ligand *trans* to the pyrazole, these signals are found at 19.25 ppm ($^3J_{HP}$ = 15.5 Hz) and 331.7

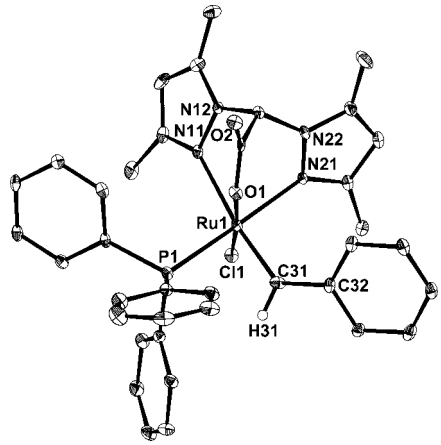

Figure 13. Molecular structure of [Ru(bdmpza)Cl(=CHPh)(PPh_3)] (**9a**) with thermal ellipsoids drawn at the 50% probability level. Hydrogen atoms and solvent molecules are omitted for clarity.

Table 2. Selected Bond Lengths (Å) and Angles (deg) of the Benzylidene Complexes 7b and 9a

7b		**9a**	
Ru−O1	2.200(2)	Ru−O1	2.079(3)
Ru−N21	2.123(3)	Ru−N21	2.157(4)
Ru−C3	1.886(4)	Ru−C31	1.895(5)
Ru−Cl	2.4102(13)	Ru−Cl	2.4065(13)
Ru−P	2.4086(11)	Ru−P	2.3094(16)
Ru−N11	2.111(3)	Ru−N11	2.271(4)
C3−C4	1.483(5)	C31−C32	1.479(8)
O1−Ru−C3	175.48(12)	O1−Ru−C31	96.87(19)
O1−Ru−Cl	87.13(7)	O1−Ru−Cl	173.47(11)
O1−Ru−N11	87.20(9)	O1−Ru−N11	84.43(15)
N21−Ru−C3	93.49(13)	N21−Ru−C31	92.9(2)
N21−Ru−P	169.66(7)	N21−Ru−P	174.13(11)
N21−Ru−N11	84.42(10)	N21−Ru−N11	79.70(16)
C3−Ru−Cl	90.22(11)	C31−Ru−Cl	89.64(16)
C3−Ru−P	95.81(11)	C31−Ru−P	86.82(19)
C3−Ru−N11	95.06(13)	C31−Ru−N11	172.4(2)
Cl−Ru−P	86.21(3)	Cl−Ru−P	93.09(5)
Cl−Ru−N11	171.98(7)	Cl−Ru−N11	89.20(11)
Ru−C3−C4	132.0(3)	Ru−C31−C32	130.0(4)

ppm ($^2J_{CP}$ = 19.8 Hz), whereas for complex **9b**, the isomer with the carbene ligand *trans* to the carboxylate, these signals were observed at 18.38 ppm ($^3J_{HP}$ = 12.0 Hz) and 335.8 ppm. These data agree very well with the respective data we discussed above. Crystals of the isomer **9a** were obtained from a CH_2Cl_2 solution layered with *n*-hexane. The X-ray structure analysis confirms the isomer structure **9a** (carbene ligand *trans* to the pyrazole) (Figure 13). The ^{31}P NMR resonance of **8** (39.6 ppm) is like that of **9a** (38.1 ppm). The ^{31}P NMR signal of **9b** is shifted to higher field by 6.6 ppm and occurs at 33.0 ppm. This is exactly where the signal of [RuCl(Tp)(=CHPh)(PCy_3)] (33.64 ppm) was found also.[7]

During the synthesis of complexes **9a** and **9b**, the rather crude complex [$RuCl_2$(=CHPh)(PPh_3)$_2$][28] may be used as a precursor almost without any workup, since a column chromatography step was applied for the purification and separation of the complex isomers **9a** and **9b**, anyway.

Molecular Structures of 7b and 9a. As depicted in Figures 12 and 13 (Table 2), both types of isomers have been crystallized in the case of the benzylidene complexes. The triphenylphosphine complex **9a** is of type A, and the analogous tricyclohexylphosphine complex **7b** is of type B. Thus, we decided to take a closer look at the different *trans* influences. First of all, the Ru−C_α bond lengths are almost the same [**7b**: 1.886(4) Å; **9a**: 1.895(5) Å]. These distances are also similar to the Ru−C_α distance of the six-coordinate benzylidene complex [Ru(Tp)(=CHPh)(H_2O)(PCy_3)][BF_4] [1.878(4) Å].[7] Even the Ru−C_α distance of the five-coordinate complex [$RuCl_2$(=CHPh-*p*-Cl)(PCy_3)$_2$] is only slightly shorter [1.839(3) Å].[28] As one might assume, all these bonds are shorter compared to the Ru−C_α bond distance in the aminocarbene complex **4** [1.988(3) and 1.982(3) Å] (see Table 1). This agrees well with the mesomeric structures of Fischer-type aminocarbene complexes, which we depict in Figure 1.

The bond lengths of the Ru−N bonds *trans* to the phosphine ligands are almost identical for the two PCy_3 complexes **7b** [2.123(3) Å] and [Ru(Tp)(=CHPh)(H_2O)(PCy_3)][BF_4] [2.129(3) Å]. That of the PPh_3 complex **9a** is slightly larger [2.157(4) Å].

In the case of the Ru−P bond lengths the situation is reversed. The complexes [Ru(bdmpza)Cl(=CHPh)(PCy_3)] (**7b**) [2.4086(11) Å] and [Ru(Tp)(=CHPh)(H_2O)(PCy_3)][BF_4] [2.3822(13) Å][7] exhibit rather long Ru−P distances due to the large cone angle of the PCy_3 ligand. Complex **9a**, with the less bulky PPh_3 ligand, exhibits a Ru−P distance of 2.3094(16) Å.

The ruthenium pyrazole bonds *trans* to a benzylidene ligand are considerably affected by the *trans* influence of the benzylidene ligand. This becomes rather obvious in the respective Ru−N distances of complex **9a** [*d*(Ru−N1) = 2.271(4) Å] and the Tp complex [Ru(Tp)(=CHPh)(H_2O)(PCy_3)][BF_4] [2.200(4) Å].[7] These distances are notably longer than those mentioned above for the *trans* coordination of a phosphine and also for **7b**, where a chlorido ligand is coordinated *trans* to the second pyrazole ring [*d*(Ru−N11) = 2.111(3) Å].

Metathesis Reaction Tests. As mentioned above, there have been reports on the catalytic activity regarding olefin metathesis also for coordinatively saturated 18-VE ruthenium benzylidene complexes. For example Sanford et al. observed activity in the case of the Tp complex [RuCl(Tp)(=CHPh)(PCy_3)][7] that is very similar to the bpza class complexes we reported on here. Therefore, the activity of some of the complexes has been tested in RCM of diethyl diallylmalonate. This RCM is a convenient and frequently used test reaction to compare the activities of different ruthenium-based metathesis catalysts.[35] We found that a phosphine scavenger[36] is necessary to observe acceptable metathesis activity at all. This means that apart from the different heteroscorpionate ligands all potential precatalysts presented in this report will end as the same catalyst after an initiation step. Therefore, we focused on complexes **6** and a mixture of **7a** and **7b** in our RCM test.

Almost no metathesis reaction was observed in CH_2Cl_2 as solvent, neither with nor without phosphine scavenger. If benzene was used as solvent and by applying reflux conditions, up to 92% RCM yield was obtained after 12 h by using complex **6** as catalyst. After addition of CuCl as phosphine scavenger 97% RCM product was achieved within 2 h in the case of the isomer mixture **7a/b** (see Table 3).

It is noteworthy that without a phosphine scavenger the bpza complex **6** is more active than the bdmpza complexes **7a/b**. This is quite surprising since the more bulky bdmpza ligand usually facilitates the dissociation of the phosphine ligand.[10] Obviously, this does not compensate the missing phosphine scavenger. Thus, we assume that this steric hindrance in **7a/b** affects also the coordination of the diethyl diallylmalonate during the catalytic cycle.

(36) Ulman, M.; Grubbs, R. H. *J. Org. Chem.* **1999**, *64*, 7202–7207.

Table 3. Results of the Metathesis Catalysis Tests[a]

precatalyst	CuCl added	reaction time [h]	yield [%]
6	no	3	39
		6	60
		12	92
	yes	1	10
		3	85
		6	95
7a/b	no	3	10
		6	41
		12	62
	yes	1	90
		2	97

[a] Grubbs' catalysts of first and second generation exhibit much higher activity in milder reaction conditions.[35]

Conclusion

Several neutral aminocarbene and benzylidene ruthenium complexes bearing the N,N,O heteroscorpionate ligands bpza and bdmpza have been synthesized. The addition of ammonia and NH_2Me to vinylidene and also allenylidene ligands takes place and is quite fast in most cases, while no reaction was observed with alcohols or the secondary amine $NHMe_2$. DFT calculations and experimental results indicate that the addition of methylamine to the vinylidene ligand proceeds via a direct mechanism with a deprotonation step and subsequent protonation. According to the DFT calculations key intermediates in these addition reactions are strongly controlled by intramolecular hydrogen bridges. This might explain why an addition of alcohols or secondary amines such as $NHMe_2$ is not successful, since their only proton is caught in these hydrogen bridges.

Furthermore, various octahedral ruthenium benzylidene complexes bearing the heteroscorpionate bpza and bdmpza ligands have been obtained from ruthenium benzylidene complexes $[RuCl_2(=CHPh)(PR_3)_2]$. These benzylidene complexes exhibit either a single isomer in the case of the bpza ligand or mixtures of two isomers for bdmpza. Two-dimensional NMR analyses and X-ray structure determinations revealed the geometries of the complexes as type A (benzylidene ligand *trans* to a pyrazole N-donor) or type B (benzylidene ligand *trans* to a carboxylate O-donor).

These benzylidene complexes show some activity in olefin metathesis reactions, tested by the RCM of diethyl diallylmalonate. The rather low activity increases when the remaining phosphine is released either by harsh reflux conditions or by applying a phosphine scavenger. First catalytic tests indicate that the activity depends on the nature of the heteroscorpionate ligand.

Experimental Section

All experiments were carried out with Schlenk techniques under an atmosphere of argon or N_2. Solvents were dried by distillation over suitable drying agents [THF, Et_2O: Na; *n*-pentane, *n*-hexane: $LiAlH_4$; CH_2Cl_2: CaH_2] prior to use and were stored under N_2. Flash chromatography was carried out on silica gel 60. IR: Biorad FTS 60, CaF_2 cuvets (0.5 mm). ^1H NMR and ^{13}C NMR: Varian Unity Inova 400 and Bruker DRX 600 Avance. ^{31}P NMR: Varian Unity Inova 400. 2D NMR experiments: Varian Unity Inova 400 and Bruker DRX 600 Avance. $^1H-^{31}P$-HMBC experiments: Varian Unity Inova 400. δ values relative to TMS (^1H), solvent peaks (^{13}C), or triphenylphosphine -4.72 ppm as internal standard (^{31}P). FAB-MS: modified Finnigan MAT 312. GC: ThermoFinnigan TRACE GC/AS 2000. Elemental analyses: Analytical Laboratory of the Fachbereich Chemie, Universität Konstanz. Diffractometer for X-ray structure determination: Stoe IPDS II and modified Siemens P4 diffractometer.

NH_3, NH_2Me, $NHMe_2$, KO^{t}Bu, PhCHN-$NHSO_2$Tol, and Grubbs' catalyst (first generation) were used as purchased. Hbdmpza, Hbpza, and $PhCHN_2$ were prepared according to the literature.[2,4,37] The potassium salts K[bpza] and K[bdmpza] were synthesized by reacting the acids with KO^{t}Bu and collecting the salts. $[RuCl_2(=CHPh)(PPh_3)]$ was synthesized according to the literature but was used without any purification.[28] The syntheses of [Ru(bdmpza)Cl(=C=CHTol)(PPh_3)] (**1**) and [Ru(bdmpza)Cl(=C=C=CTol$_2$)(PPh_3)] (**2a**, **2b**) have been reported recently.[10] For differentiation of the NMR data the pyrazole signals of the bdmpza ligand next to the PPh_3 ligand are marked with a prime.

Method A: General Procedure for the Reaction of the Cumulenylidene Complexes 1−2b with Amines Yielding Complexes 3−5b. To a solution or suspension of the cumulenylidene complex[10] in THF was added a solution of the amine. When the reaction was finished, the solvent was evaporated in vacuo and the residue was dissolved in CH_2Cl_2 and precipitated with *n*-hexane. The solvent was decanted and the products were dried in vacuo.

[Ru(bdmpza)Cl(=C(NH$_2$)CH$_2$Tol)(PPh$_3$)] (3). Reaction of [Ru(bdmpza)Cl(=C=CHTol)(PPh_3)] (**1**, 0.200 g, 0.262 mmol) in THF with gaseous NH_3 for 10 min according to method A afforded complex [Ru(bdmpza)Cl(=C(NH_2)CH_2Tol)(PPh_3)] (**3**) as a yellow, crystalline powder.

Yield: 0.167 g (82%). Mp: 193 °C dec. IR (CH_2Cl_2): $\tilde{\nu}$ 1657 s (CO_2^-), 1642 sh, 1605 w, 1564 w (C=N), 1513 w, 1483 w, 1462 w, 1434 w, 1419 w cm^{-1}. FAB-MS (NBOH matrix): *m/z* (relative intensity) 779 (100) [M^+], 744 (18) [M^+ − Cl], 611 (10) [M^+ − C(NH_2)CH_2Tol]. Anal. Calcd for $C_{39}H_{41}ClN_5O_2PRu$ (779.27): C, 60.11; H, 5.30; N, 8.99. Found: C, 60.10; H, 5.28; N, 8.98. UV/vis (CH_2Cl_2): λ_{max} (log ε) 234 (4.05), 268 (3.81), 275 (3.80), 305 (3.84) nm. ^1H NMR (CD_2Cl_2, 400 MHz): δ (ppm) 1.87 (s, 3H, Me$^{3'}$), 2.33 (s, 3H, Me^{Tol}), 2.34 (s, 3H, Me^3), 2.49 (s, 3H, Me^5), 2.54 (s, 3H, Me$^{5'}$), 3.88 and 4.21 (AB system, J_{AB} = 19.2 Hz, 2H, CH_2), 5.83 (s, 1H, H$^{4'}$), 6.04 (s, 1H, H^4), 6.58 (s, 1H, CH), 6.94 (d, $^3J_{HH}$ = 7.6 Hz, 2H, *o*-Tol), 7.17 (d, $^3J_{HH}$ = 7.6 Hz, 2H, *m*-Tol), 7.27 (m, 6H, *m*-PPh_3), 7.36 (m, 9H, *p*-PPh_3, *o*-PPh_3), 8.05 (br, 1H, 1 × NH), 8.74 (br, 1H, 1 × NH). ^{13}C NMR (CD_2Cl_2, 100 MHz): δ (ppm) 10.9 (Me^5), 10.8 (Me$^{5'}$), 13.8 (Me^3), 13.8 (Me$^{3'}$), 20.5 (Me^{Tol}), 53.0 (C$_\beta$), 69.1 (CH), 108.1 (C$^{4'}$), 108.4 (C^4), 127.2 (m, $^3J_{CP}$ = 8.9 Hz, *m*-PPh_3), 129.4 (*m*-Tol), 128.7 (*p*-PPh_3), 129.8 (*o*-Tol), 131.9 (*i*-Tol), 133.9 (d, $^2J_{CP}$ = 9.1 Hz, *o*-PPh_3), 136.7 (*p*-Tol), 134.8 (d, $^1J_{CP}$ = 39.3 Hz, *i*-PPh_3), 140.5 (C^5), 141.1 (C$^{5'}$), 153.9 (C^3), 155.8 (C$^{3'}$), 167.1 (CO_2^-), 271.2 (d, $^2J_{CP}$ = 14.6 Hz, C$_\alpha$). ^{31}P NMR ($CDCl_3$, 161.8 MHz): δ (ppm) 50.4.

[Ru(bdmpza)Cl(=C(NHMe)CH$_2$Tol)(PPh$_3$)] (4). Reaction of [Ru(bdmpza)Cl(=C=CHTol)(PPh_3)] (**1**, 0.200 g, 0.262 mmol) with a NH_2Me solution in THF (0.2 mol·L^{-1}, 2.6 mL, 0.53 mmol) for 5 min according to method A afforded complex [Ru(bdmpza)Cl(=C(NHMe)CH_2Tol)(PPh_3)] (**4**) as a yellow, crystalline powder.

Yield: 0.186 g (89%). Mp: 159 °C dec. IR (CH_2Cl_2): $\tilde{\nu}$ 1656 s (CO_2^-), 1641 sh, 1565 w (C=N), 1528 w, 1512 w, 1482 w, 1463 w, 1436 w, 1433 w, 1419 w cm^{-1}. FAB-MS (NBOH matrix): *m/z* (relative intensity) 793 (100) [M^+], 758 (11) [M^+ − Cl], 646 (38) [M^+ − C(NHMe)CH_2Tol]. Anal. Calcd for $C_{40}H_{43}ClN_5O_2PRu$ (793.30): C, 60.56; H, 5.46; N, 8.83. Found: C, 60.65; H, 5.50; N, 8.96. UV/vis (CH_2Cl_2): λ_{max} (log ε) 237 (4.36), 267 (3.87), 274 (3.86), 319 (3.93) nm. ^1H NMR (CD_2Cl_2, 400 MHz): δ (ppm) 1.69 (s, 3H, Me^3), 1.76 (s, 3H, Me$^{3'}$), 2.17 (s, 3H, Me^{Tol}) 2.37 (s, 3H, Me^5), 2.48 (s, 3H, Me$^{5'}$), 3.16 (d, *J* = 3.6 Hz, 3H, NMe), 3.29 and 4.00 (AB system, J_{AB} = 12.4 Hz, 2H, CH_2), 5.46 (s, 1H, H^4), 5.74 (s, 1H, H$^{4'}$), 6.49 (s, 1H, CH), 6.63 (d, $^3J_{HH}$ = 7.20 Hz, 2H, *o*-Tol), 6.72 (d, $^3J_{HH}$ = 7.20 Hz, 2H, *m*-Tol), 7.24 (m, 6H, *m*-PPh_3), 7.31

(37) Wulfman, D. S.; Yousefian, S.; White, J. M. *Synth. Commun.* **1998**, *18*, 2349–2352.

(m, 3H, *p*-PPh_3), 7.41 (m, 6H, *o*-PPh_3), 9.84 (s, 1H, NH). ^{13}C NMR (CD_2Cl_2, 100 MHz): δ (ppm) 11.3 (Me^5), 11.4 ($Me^{5'}$), 14.4 (Me^3), 14.6 ($Me^{3'}$), 20.9 (Me^{Tol}), 35.6 (NMe), 43.9 (C_β), 69.6 (CH), 108.5 ($C^{4'}$), 108.6 (d, $^4J_{CP}$ = 2.6 Hz, C^4), 127.6 (d, $^3J_{CP}$ = 8.8 Hz, *m*-PPh_3), 128.6 (*m*-Tol), 129.2 (*p*-PPh_3), 130.0 (*o*-Tol), 132.9 (*i*-Tol), 134.5 (d, $^2J_{CP}$ = 9.3 Hz, *o*-PPh_3), 135.3 (*p*-Tol), 136.3 (d, $^1J_{CP}$ = 38.5 Hz, *i*-PPh_3), 140.1 (C^5), 141.5 ($C^{5'}$), 155.5 (C^3), 156.0 ($C^{3'}$), 167.7 (CO_2^-), 265.1 (d, $^2J_{CP}$ = 15.3 Hz, C_α). ^{31}P NMR ($CDCl_3$, 161.8 MHz): δ (ppm) 47.0.

[Ru(bdmpza)Cl(=C(NHMe)CH=CTol$_2$)(PPh$_3$)] (5a) Carbene *trans* Pyrazole. Reaction of [Ru(bdmpza)Cl(=C=C=CTol$_2$)(PPh$_3$)] (**2a**, allenylidene *trans* pyrazole) (0.200 g, 0.231 mmol) with a solution of NH_2Me in THF (0.2 mol·L^{-1}, 6.0 mL, 1.2 mmol) for 3 min according to method A afforded complex [Ru(bdmpza)-Cl(=C(NHMe)CH=CTol$_2$)(PPh$_3$)] (**5a**, carbene *trans* pyrazole) as a brown, crystalline powder.

Yield: 0.139 g (67%). Mp: 164 °C dec. IR (CH_2Cl_2): $\tilde{\nu}$ 1656 s (CO_2^-), 1565 w (C=N), 1533 w, 1505 w, 1483 w, 1462 w, 1436 w, 1419 w cm^{-1}. FAB-MS (NBOH matrix): *m/z* (relative intensity) 895 (100) [M^+], 611 (21) [M^+ − Cl − C(NHMe)CHCTol$_2$]. Anal. Calcd for $C_{48}H_{49}ClN_5O_2PRu$ (895.43): C, 64.38; H, 5.52; N, 7.82. Found: C, 64.05; H, 5.49; N, 7.60. UV/vis (CH_2Cl_2): λ_{max} (log ε) 246 (4.36), 298 (4.09), 395 (3.51) nm. ^1H NMR (CD_2Cl_2, 400 MHz, not all expected signals resolved): δ (ppm) 1.75 (s, 3H, $Me^{3'}$), 2.15 (s, 3H, Me^3), 2.29 (s, 3H, Me^{Tol}), 2.32 (s, 3H, $Me^{Tol''}$), 2.43 (s, 3H, Me^5), 2.49 (s, 3H, $Me^{5'}$), 2.57 (d, *J* = 3.60 Hz, 3H, NMe), 5.75 (s, 1H, $H^{4'}$), 5.87 (s, 1H, H^4), 6.48 (s, 1H, CH), 6.73 (d, $^3J_{HH}$ = 8.40 Hz, 2H, *o*-Tol), 6.89 (d, $^3J_{HH}$ = 8.40 Hz, 2H, *m*-Tol), 6.91 (d, $^3J_{HH}$ = 8.80 Hz, 2H, *o*-Tol″), 7.03 (d, $^3J_{HH}$ = 7.60 Hz, 2H, *m*-Tol″), 7.22 (vt, 6H, *m*-PPh_3), 7.27 (vd, 3H, *p*-PPh_3), 7.58 (vt, 6H, *o*-PPh_3), 9.02 (br, 1H, NH). ^{13}C NMR (CD_2Cl_2, 100 MHz, not all expected signals resolved): δ (ppm) 10.8 (Me^5), 10.8 ($Me^{5'}$), 13.7 (Me^3), 13.9 ($Me^{3'}$), 20.5 ($Me^{Tol''}$), 20.6 (Me^{Tol}), 37.4 (NMe), 68.8 (CH), 108.1 ($C^{4'}$), 108.4 (d, $^4J_{CP}$ = 2.2 Hz, C^4), 127.0 (d, $^3J_{CP}$ = 8.8 Hz, *m*-PPh_3), 127.5 (*o*-Tol″), 128.1 (*m*-Tol), 128.2 (*m*-Tol″), 128.3 (*p*-PPh_3), 128.8 (*o*-Tol), 133.9 (d, $^2J_{CP}$ = 9.3 Hz, *o*-PPh_3), 135.9 (d, $^1J_{CP}$ = 38.7 Hz, *i*-PPh_3), 136.7 (*p*-Tol), 136.9 (*p*-Tol″), 137.3 (*i*-Tol), 139.8 (C^5), 140.7 (i-Tol″), 141.0 ($C^{5'}$), 154.6 (C^3), 156.0 ($C^{3'}$), 166.8 (CO_2^-), 255.3 (C_α); ^{31}P NMR ($CDCl_3$, 161.8 MHz): δ (ppm) 49.6.

[Ru(bdmpza)Cl(=C(NHMe)CH=CTol$_2$)(PPh$_3$)] (5b) Carbene *trans* Carboxylate. Reaction of [Ru(bdmpza)Cl(=C=C=CTol$_2$)-(PPh$_3$)] (**2b**, allenylidene *trans* carboxylate) (0.200 g, 0.231 mmol) with a solution of NH_2Me in THF (0.2 mol·L^{-1}, 6.0 mL, 1.2 mmol) for 18 h according to method A afforded complex [Ru-(bdmpza)Cl(=C(NHMe)CH=CTol$_2$)(PPh$_3$)] (**5b**, carbene *trans* carboxylate) as an orange, crystalline powder.

Yield: 0.162 g (78%). Mp: 179 °C dec. IR (CH_2Cl_2): $\tilde{\nu}$ 1659 s (CO_2^-), 1653 s, 1566 w (C=N), 1534 w, 1508 w, 1483 w, 1463 w, 1446 w, 1435 w, 1422 w cm^{-1}. FAB-MS (NBOH matrix): *m/z* (relative intensity) 895 (100) [M^+], 860 (29) [M^+ − Cl], 611 (47) [M^+ − Cl − C(NHMe)CHCTol$_2$]. Anal. Calcd for $C_{48}H_{49}ClN_5O_2$-PRu (895.43): C, 64.38; H, 5.52; N, 7.82. Found: C, 64.30; H, 5.70; N, 7.74. UV/vis (CH_2Cl_2): λ_{max} (log ε) 235 (4.56), 301 (4.20), 395 (3.57) nm. ^1H NMR (CD_2Cl_2, 400 MHz): δ (ppm) 1.37 (s, 3H, $Me^{3'}$), 2.16 (s, 3H, Me^3), 2.22 (s, 3H, $Me^{Tol''}$) 2.23 (d, *J* = 8.0 Hz, 3H, NMe), 2.29 (s, 3H, Me^{Tol}), 2.49 (s, 3H, $Me^{5'}$), 2.50 (s, 3H, Me^5), 5.61 (s, 1H, $H^{4'}$), 5.91 (s, 1H, H^4), 5.99 (s, 1H, H_β), 6.39 (d, $^3J_{HH}$ = 7.20 Hz, 2H, *o*-Tol), 6.51 (s, 1H, CH), 6.67 (d, $^3J_{HH}$ = 7.60 Hz, 2H, *o*-Tol″), 6.88 (d, $^3J_{HH}$ = 7.60 Hz, 2H, *m*-Tol), 6.91 (d, $^3J_{HH}$ = 8.00 Hz, 2H, *m*-Tol″), 7.28 (br, 9H, *m*-PPh_3, *p*-PPh_3), 7.72 (br, 6H, *o*-PPh_3), 8.71 (s, 1H, NH). ^{13}C NMR (CD_2Cl_2, 100 MHz): δ (ppm) 10.7 (Me^5), 11.4 ($Me^{5'}$), 13.6 (Me^3), 16.7 ($Me^{3'}$), 20.5 ($Me^{Tol''}$), 20.7 (Me^{Tol}), 36.8 (NMe), 69.1 (CH), 107.3 ($C^{4'}$), 108.7 (d, $^4J_{CP}$ = 2.6 Hz, C^4), 127.0 (*o*-Tol″), 127.6 (d, $^3J_{CP}$ = 7.6 Hz, *m*-PPh_3), 128.1 (*m*-Tol), 128.3 (*o*-Tol, *m*-Tol″), 128.4, 128.5, 133.6 (br) (*i*-PPh_3, *o*-PPh_3, *p*-PPh_3), 133.4 (C_β), 134.8 (C_γ), 136.4 (i-Tol″), 136.9 (*p*-Tol), 137.0 (*p*-Tol″), 139.5 (C^5), 140.4 (*i*-Tol), 141.6 ($C^{5'}$), 154.3 (d, $^3J_{CP}$ = 1.9 Hz, C^3), 155.6 ($C^{3'}$), 166.2 (CO_2^-), 252.1 (d, $^2J_{CP}$ = 10.1 Hz, C_α). ^{31}P NMR ($CDCl_3$, 161.8 MHz): δ (ppm) = 45.3.

Method B: General Procedure for the Syntheses of the Benzylidene Complexes 6−9b Bearing the Heteroscorpionate Ligands bpza and bdmpza. To the benzylidene complexes [$RuCl_2$(=CHPh)(PR_3)$_2$] (R = Cy, Ph)[28] was added a slight excess of the potassium salt K[bpza] or K[bdmpza], and the mixture was dissolved in CH_2Cl_2. After stirring at ambient temperature a small amount of silica was added and the solvent was removed in vacuo. The mixture was loaded on a column of silica (length 20 cm, Φ 4 cm) and the column was washed with pentane and Et_2O. The product or the isomers, respectively, were eluted using CH_2Cl_2/acetone (1:1 v/v) and finally MeOH. The fractions were evaporated in vacuo and precipitated from CH_2Cl_2 with *n*-hexane. The solvent was decanted, and the products were dried in vacuo.

[Ru(bpza)Cl(=CHPh)(PCy$_3$)] (6). Reaction of [$RuCl_2$(=CHPh)-(PCy_3)$_2$] (0.400 g, 0.486 mmol) with K[bpza] (0.123 g, 0.535 mmol) for 15 h according to method B afforded the complex [Ru(bpza)Cl(=CHPh)(PCy_3)] (**6**) as a green, crystalline powder.

Yield: 0.198 g (58%). Mp: 165 °C dec. IR (CH_2Cl_2): $\tilde{\nu}$ 1663 s (CO_2^-), 1655 s, 1447 w, 1410 w cm^{-1}. FAB-MS (NBOH matrix): *m/z* (relative intensity) 698 (42) [M^+], 662 (73) [M^+ − Cl], 572 (31) [M^+ − CHPh − Cl], 327 (100) [M^+ − CHPh − PCy_3]. Anal. Calcd for $C_{33}H_{46}ClN_4O_2PRu$ (698.24): C, 56.76; H, 6.64; N, 8.02. Found: C, 56.89; H, 6.67; N, 7.42. UV/vis (CH_2Cl_2): λ_{max} (log ε) 265 (3.66), 356 (3.49) nm. ^1H NMR (CD_2Cl_2, 400 MHz): δ (ppm) 0.96−1.91 (33H, PCy_3), 6.20 (s, 1H, H^4), 6.29 (s, 1H, $H^{4'}$), 6.54 (s, 1H, $H^{3'}$), 6.79 (s, 1H, H^3), 6.91 (vd, 2H, *o*-Ph), 7.13 (vt, 2H, *m*-Ph), 7.55 (vt, 1H, *p*-Ph), 7.95 (br, 1H, CH), 8.21 (br, 1H, H^5), 8.37 (br, 1H, $H^{5'}$), 20.09 (d, $^3J_{HP}$ = 8.00 Hz, 1H, H_α); ^{13}C NMR (CD_2Cl_2, 100 MHz): δ (ppm) 26.3 (PCy_3), 27.4 (d, J_{CP} = 10.1 Hz, PCy_3), 27.7 (d, J_{CP} = 9.5 Hz, PCy_3), 28.1 (2 × PCy_3), 34.0 (d, J_{CP} = 19.1 Hz, PCy_3), 75.3 (CH), 107.4 (d, $^4J_{CP}$ = 1.8 Hz, C^4), 107.8 ($C^{4'}$), 128.8 (*m*-Ph), 129.9 (*o*-Ph), 130.6 (*p*-Ph), 132.3 (C^5), 134.3 ($C^{5'}$), 143.4 (C^3), 146.3 ($C^{3'}$), 150.4 (*i*-Ph), 165.0 (CO_2^-), 328.3 (C_α); ^{31}P NMR ($CDCl_3$, 161.8 MHz): δ (ppm) 26.6.

[Ru(bdmpza)Cl(=CHPh)(PCy$_3$)] (7a, 7b). Reaction of [$RuCl_2$(=CHPh)(PCy_3)$_2$] (0.400 g, 0.486 mmol) with K[bdmpza] (0.153 g, 0.535 mmol) for 15 h according to method B afforded two isomers of complex [Ru(bdmpza)Cl(=CHPh)(PCy_3)] (**7a**, **7b**) as a green, crystalline powder.

Yield: 0.205 g (56%). Mp: 157 °C dec. IR (CH_2Cl_2): $\tilde{\nu}$ 1659 s (CO_2^-), 1643 sh, 1564 w (C=N), 1460 w, 1448 w, 1420 w cm^{-1}. FAB-MS (NBOH matrix): *m/z* (relative intensity) 754 (100) [M^+], 719 (26) [M^+ − Cl]. Anal. Calcd for $C_{37}H_{54}ClN_4O_2PRu$ (754.35): C, 58.91; H, 7.22; N, 7.43. Found: C, 58.75; H, 7.40; N, 7.28. UV/vis (CH_2Cl_2): λ_{max} (log ε) 235 (4.41), 305 (3.86) nm. **7a** (benzylidene *trans* to pyrazole): ^1H NMR (CD_2Cl_2, 400 MHz): δ (ppm) 0.99 (m, 5H, PCy_3) 1.20 (m, 4H, PCy_3), 1.42 (s, 3H, Me^3), 1.60 (m, 17H, PCy_3), 1.90 (m, 4H, PCy_3), 2.04 (br, 3H, PCy_3), 2.51 (s, 3H, Me^5), 2.56 (s, 3H, $Me^{5'}$), 3.05 (s, 3H, $Me^{3'}$), 5.75 (s, 1H, H^4), 6.25 (s, 1H, $H^{4'}$), 6.67 (s, 1H, CH), 7.31 (vt, 2H, *m*-Ph), 7.68 (vt, 1H, *p*-Ph), 7.78 (vd, 2H, *o*-Ph), 20.47 (d, $^3J_{HP}$ = 11.60 Hz, 1H, H_α). ^{13}C NMR (CD_2Cl_2, 100 MHz): δ (ppm) 10.8 (Me^5), 10.9 ($Me^{5'}$), 12.7 (Me^3), 15.9 ($Me^{3'}$), 26.2 (PCy_3), 27.7 (d, J_{CP} = 5.0 Hz, PCy_3), 27.8 (d, J_{CP} = 6.6 Hz, PCy_3), 28.6 (s, PCy_3), 28.9 (s, PCy_3), 37.5 (d, J_{CP} = 19.1 Hz, PCy_3), 69.1 (CH), 107.9 (d, $^4J_{CP}$ = 2.3 Hz, C^4), 109.0 ($C^{4'}$), 128.9 (*m*-Ph), 129.8 (*o*-Ph), 130.1 (*p*-Ph), 140.1 (d, $^5J_{CP}$ = 1.1 Hz, C^5), 141.3 ($C^{5'}$), 152.3 (d, $^3J_{CP}$ = 1.8 Hz, C^3), 153.2 (*i*-Ph), 155.2 ($C^{3'}$), 165.9 (CO_2^-), 326.4 (C_α). ^{31}P NMR ($CDCl_3$, 161.8 MHz): δ (ppm) 25.6. **7b** (benzylidene *trans* to carboxylate): ^1H NMR (CD_2Cl_2, 400 MHz): δ (ppm) 0.83−1.53 (br, 17H, PCy_3), 1.26 (s, 3H, $Me^{3'}$), 1.45 (s, 3H, Me^3), 1.54−2.09 (br, 16H, PCy_3), 2.52 (s, 3H, Me^5), 2.60 (s, 3H, $Me^{5'}$), 5.79 (s, 1H, H^4), 5.88 (s, 1H, $H^{4'}$), 6.52 (vd, 1H, *o*-Ph), 6.67 (s, 1H, CH), 6.86 (vt, 1H, *m*-Ph),7.43 (vt, 1H, *p*-Ph), 7.58 (vt, 1H, *m*-Ph),

Table 4. Structure Determination Details of Compounds 4, 6, 7b, and 9a

	4	6	7b	9a
empirical formula	$2 \times C_{40}H_{43}Cl_2N_5O_2PRu \times CH_2Cl_2$	$C_{33}H_{46}ClN_4O_2PRu \times 1.5\ CH_2Cl_2$	$C_{37}H_{54}ClN_4O_2PRu \times 0.5\ C_5H_{12} \times 1.5\ CH_2Cl_2$	$C_{37}H_{36}ClN_4O_2PRu \times 2\ CH_2Cl_2$
fw	1671.49	825.62	917.79	906.04
cryst color/habit	orange block	green plate	green block	green plate
cryst syst	monoclinic	monoclinic	monoclinic	monoclinic
space group, Z	$P2_1/c$, 4	$P2_1/c$, 4	$C2/c$, 8	$P2_1/n$, 4
a [Å]	18.0582(8)	15.350(3)	32.805(10)	14.278(3)
b [Å]	22.6925(9)	10.613(2)	14.103(7)	18.997(4)
c [Å]	18.8519(9)	25.671(5)	20.868(9)	16.217(3)
α [deg]	90	90	90	90
β [deg]	92.771(4)	98.78(3)	110.59(3)	115.07(3)
γ [deg]	90	90	90	90
V [Å^3]	7716.2(6)	4133.1(14)	9038(6)	3984.3(17)
θ [deg]	3.33−25.82	3.30−23.77	2.02−27.00	3.33−23.69
h min, max.	−21, 21	−16, 17	−1, 41	−16, 14
k min, max.	−27, 27	−11, 11	−18, 1	0, 21
l min, max.	−23, 23	−28, 28	−26, 25	0, 18
μ(Mo Kα) [mm^{-1}]	0.629	0.71	0.656	0.809
cryst size [mm]	0.4 × 0.3 × 0.2	0.4 × 0.283 × 0.15	0.5 × 0.5 × 0.4	0.50 × 0.37 × 0.20
D_c [gcm^{-3}]	1.439	1.327	1.349	1.510
T [K]	100(2)	100(2)	188(2)	100(2)
reflns collected	85 021	26 071	11 221	40 591
indep reflns	14 553	5757	9840	5923
obsd reflns (>2σI)	11 046	3540	7195	4258
params	934	446	499	469
restraints	0	26	8	0
wt param a	0.0354	0.1188	0.0430	0.0847
wt param b	6.8592	0	17.3903	0
R_1/wR_2 (obsd)	0.0438/0.0858	0.0688/0.1719	0.0470/0.1032	0.0484/0.122
R_1/wR_2 (overall)	0.0698/0.0945	0.1185/0.1955	0.0749/0.1133	0.0657/0.1256
diff peak/hole [e/Å^3]	0.607/−0.687	1.815/−0.829	0.679/−0.744	1.322/−1.571
goodness-of-fit on F^2	1.023	0.976	1.014	0.923

7.87 (vd, 1H, *o*-Ph), 20.45 (d, $^3J_{HP}$ = 8.80 Hz, 1H, H$_\alpha$). ^{13}C NMR (CD_2Cl_2, 100 MHz): δ (ppm) 10.7 (Me^5), 11.4 (Me$^{5'}$), 13.3 (Me^3), 15.9 (Me$^{3'}$), 26.6 (PCy$_3$), 28.0 (br, PCy$_3$), 29.1 (br, PCy$_3$), 35.7 (d, J_{CP} = 14.0 Hz, PCy$_3$), 69.4 (CH), 107.8 (d, $^4J_{CP}$ = 2.6 Hz, C^4), 108.2 (C$^{4'}$), 127.9 (*o*-Ph), 128.9 (*o*-Ph), 129.0 (*m*-Ph), 192.1 (*m*-Ph), 130.0 (*p*-Ph), 140.0 (C^5), 142.1 (C$^{5'}$), 152.6 (C^3), 152.6 (*i*-Ph), 153.8 (C$^{3'}$), 165.0 (CO_2^-), 325.7 (d, $^2J_{CP}$ = 15.7 Hz, C$_\alpha$). ^{31}P NMR ($CDCl_3$, 161.8 MHz): δ (ppm) 19.7.

[Ru(bpza)Cl(=CHPh)(PPh$_3$)] (8). Reaction of impure [$RuCl_2$(=CHPh)(PPh_3)$_2$] (1.00 g) with bpzaK (0.293 g, 1.27 mmol) for 15 h according to method B afforded the complex [Ru(bpza)Cl(=CHPh)(PPh_3)] (**8**) as a green, crystalline powder.

Yield: 0.314 g (36%) over two steps. Mp: 151 °C dec. IR (CH_2Cl_2): $\tilde{\nu}$ 1662 s (CO_2^-), 1653 s, 1447 w, 1411 w cm^{-1}. FAB-MS (NBOH matrix): *m*/*z* (relative intensity) 680 (25) [M$^+$], 645 (100) [M$^+$ − Cl], 590 (16) [M$^+$ − CHPh]. Anal. Calcd for $C_{33}H_{28}ClN_4O_2PRu$ (680.10): C, 58.28; H, 4.15; N, 8.24. Found: C, 58.32; H, 4.23; N, 8.20. UV/vis (CH_2Cl_2): λ_{max} (log ε) 246 (4.25), 373 (3.88) nm. ^{1}H NMR (CD_2Cl_2, 600 MHz): δ (ppm) 5.50 (s, 1H, H$^{3'}$) 5.81 (s, 1H, H$^{4'}$), 6.25 (s, 1H, H^4), 6.62 (vd, 2H, *o*-Ph), 6.87 (s, 1H, H^3), 7.05 (vt, 2H, *m*-Ph), 7.34 (m, 6H, *m*-PPh$_3$), 7.39 (m, 3H, *p*-PPh$_3$), 7.52 (m, 1H, *p*-Ph), 7.69 (m, 6H, *o*-PPh$_3$), 7.94 (s, 1H, CH), 8.22 (s, 2H, H^5 + H$^{5'}$), 18.27 (d, $^3J_{HP}$ = 12.00 Hz, 1H, H$_\alpha$). ^{13}C NMR (CD_2Cl_2, 150 MHz): δ (ppm) 75.5 (CH), 107.3 (C$^{4'}$), 107.6 (d, $^4J_{CP}$ = 1.9 Hz, C^4), 127.7 (d, $^3J_{CP}$ = 9.7 Hz, *m*-PPh$_3$), 128.7 (*m*-Ph), 129.6 (*p*-PPh$_3$), 130.3 (*o*-Ph), 131.6 (*p*-Ph), 131.9 (d, $^1J_{CP}$ = 38.1 Hz, *i*-PPh$_3$), 132.5 (C^5), 133.6 (C$^{5'}$), 134.1 (d, $^2J_{CP}$ = 9.5 Hz, *o*-PPh$_3$), 143.7 (C^3), 146.3 (C$^{3'}$), 150.2 (*i*-Ph), 165.8 (CO_2^-), 337.8 (C$_\alpha$). ^{31}P NMR ($CDCl_3$, 161.8 MHz): δ (ppm) 39.6.

[Ru(bdmpza)Cl(=CHPh)(PPh$_3$)] (9a, 9b). Reaction of crude [$RuCl_2$(=CHPh)(PPh_3)$_2$] (1.00 g) with K[bdmpza] (0.364 g, 1.27 mmol) for 15 h according to method B afforded two isomers of complex [Ru(bdmpza)Cl(=CHPh)(PPh_3)] (**9a**, **9b**) as a green, crystalline powder.

Yield: 0.318 g (34%) over two steps. Mp: 188 °C. IR (CH_2Cl_2): $\tilde{\nu}$ 1661 s (CO_2^-), 1643 sh, 1564 w (C=N), 1483 w, 1462 w, 1449 w, 1435 w, 1420 w cm^{-1}. FAB-MS (NBOH matrix): *m*/*z* (relative intensity) 736 (100) [M$^+$], 701 (90) [M$^+$ − Cl], 646 (85) [M$^+$ − CHPh]. Anal. Calcd for $C_{37}H_{36}ClN_4O_2PRu$ (736.20): C, 60.36; H, 4.93; N, 7.61. Found: C, 60.50; H, 5.19; N, 7.58. UV/vis (CH_2Cl_2): λ_{max} (log ε) 246 (4.32), 378 (3.99) nm. **9a** (benzylidene *trans* to pyrazole): ^{1}H NMR (CD_2Cl_2, 400 MHz): δ (ppm) 1.29 (s, 3H, Me^3), 2.15 (s, 3H, Me$^{3'}$), 2.58 (s, 6H, Me^5, Me$^{5'}$), 5.80 (s, 1H, H^4), 6.01 (s, 1H, H$^{4'}$), 6.81 (s, 1H, CH), 7.22 (br, 6H, *m*-PPh$_3$), 7.26 (br, 6H, *o*-PPh$_3$), 7.33 (br, 2H, *m*-Ph), 7.35 (br, 3H, *p*-PPh$_3$), 7.70 (br, 1H, *p*-Ph), 7.72 (br, 2H, *o*-Ph), 19.25 (d, $^3J_{HP}$ = 15.5 Hz, 1H, H$_\alpha$). ^{13}C NMR (CD_2Cl_2, 100 MHz): δ (ppm) 11.4 (Me$^{5'}$), 11.5 (Me^5), 13.3 (Me^3), 14.2 (Me$^{3'}$), 69.8 (CH), 108.7 (d, $^4J_{CP}$ = 2.7 Hz, C^4), 109.2 (C$^{4'}$), 127.8 (d, $^4J_{CP}$ = 9.5 Hz, *m*-PPh$_3$), 129.5 (*m*-Ph), 129.9 (d, $^3J_{CP}$ = 2.0 Hz, *p*-PPh$_3$), 130.7 (*o*-Ph), 131.6 (*p*-Ph), 134.4 (d, $^2J_{CP}$ = 9.4 Hz, *o*-PPh$_3$), 133.0 (d, $^1J_{CP}$ = 44.5 Hz, *i*-PPh$_3$), 140.9 (C^5), 141.6 (C$^{5'}$), 153.6 (d, $^3J_{CP}$ = 2.1 Hz, C^3), 154.1 (*i*-Ph), 156.6 (C$^{3'}$), 167.0 (CO_2^-), 331.7 (d, $^2J_{CP}$ = 19.8 Hz, C$_\alpha$); ^{31}P NMR ($CDCl_3$, 161.8 MHz): δ (ppm) 38.1. **9b** (benzylidene *trans* to carboxylate): ^{1}H NMR (CD_2Cl_2, 400 MHz): δ (ppm) 0.38 (s, 3H, Me$^{3'}$), 1.38 (s, 3H, Me^3), 2.62 (s, 3H, Me^5), 2.67 (s, 3H, Me$^{5'}$), 5.67 (s, 1H, H$^{4'}$), 5.86 (s, 1H, H^4), 6.43 (br, 1H, Ph), 6.89 (s, 1H, CH), 6.81 (br, 1H, Ph), 7.13 (br, 1H, Ph), 7.32 (br, 6H, *m*-PPh$_3$), 7.38 (vd, 3H, *p*-PPh$_3$), 7.56 (br, 1H, Ph), 7.74 (br, 6H, *o*-PPh$_3$), 7.82 (br, 1H, Ph), 18.38 (d, $^3J_{HP}$ = 12.0 Hz, 1H, H$_\alpha$). ^{13}C NMR (CD_2Cl_2, 100 MHz): δ (ppm) 10.8 (Me^5), 11.4 (Me$^{5'}$), 13.2 (Me^3), 13.6 (Me$^{3'}$), 69.6 (CH), 107.9 (C$^{4'}$), 108.1 (d, $^4J_{CP}$ = 2.6 Hz, C^4), 127.8 (d, $^4J_{CP}$ = 9.5 Hz, *m*-PPh$_3$), 128.8 (Ph), 129.3 (*p*-PPh$_3$, Ph), 130.9 (Ph), 133.9 (br, *o*-PPh$_3$), 133.5 (d, $^1J_{CP}$ = 44.9 Hz, *i*-PPh$_3$), 140.3 (C^5), 141.9 (C$^{5'}$), 152.1 (*i*-Ph), 153.4 (C^3), 153.9 (C$^{3'}$), 165.7 (CO_2^-), 335.8 (C$_\alpha$). ^{31}P NMR ($CDCl_3$, 161.8 MHz): δ (ppm) 33.0.

Catalytic Tests for RCM of Diethyl Diallylmalonate. In a two-necked flask (10 mL) equipped with condenser, argon inlet, and silicone membrane were added dodecane and diethyl diallylmalonate (10 μL 4.13 × 10^{-5} mol) to benzene (2 mL). The samples were heated to reflux, and catalyst (2.06 × 10^{-6} mol) and the additive CuCl (1.03 × 10^{-5} mol) were subsequently added. The

composition of the reaction mixture was followed by gas chromatography for 12 h or until reaction completion. The results are summarized in Table 3.

Calculations. All DFT calculations and full geometry optimizations were carried out using Jaguar 6.0012[38] running on Linux 2.4.18-14smp on five Athlon MP 2800+ dual-processor workstations (Beowulf cluster) parallelized with MPICH 1.2.4. Starting geometries were obtained from X-ray structures or MM+ optimizations. Complete geometry optimizations were carried out on the implemented LACVP* basis set (ECP for heavy atoms, N31G6* for all other atoms) and the BP86 density functional. The second derivatives were calculated in all cases to ensure that true minima were found by the absence of large negative frequencies. Transition states were approximated by a geometry scan along the corresponding atom−atom distances. The maximum-energy structures from the geometry scan were used as input geometry for the transition state optimization. Second derivatives were used for transition state validation (only one large negative frequency, $\mathbf{II}_E$: -105 cm^{-1}, $\mathbf{II}_P$: -88 cm^{-1}, $\mathbf{IV}_E$: -1736 cm^{-1}, $\mathbf{IV}_P$: -1628 cm^{-1}). Structure pictures were prepared with the program Diamond 3.1e.[39]

X-ray Structure Determinations. Single crystals of **4**, **6**, **7b**, and **9a** were mounted with Paratone-N onto a glass fiber. A Stoe IPDS II diffractometer (**4**, **6**, **9a**) and a modified Siemens P4 diffractometer (**7b**) were used for data collection (graphite monochromator, Mo Kα radiation, $\lambda = 0.71073$ Å). The structures were solved by using either direct methods or Patterson methods (Siemens SHELXS-97[40]) and refined with full-matrix least-squares against F^2 (Siemens SHELXL-97[40]). A weighting scheme was applied in the last steps of the refinement with $w = 1/[\sigma^2(F_o^2) + (aP)^2 + bP]$ and $P = [2F_c^2 + \mathrm{Max}(F_o^2,0)]/3$. Most hydrogen atoms were included in their calculated positions and refined in a "riding model". The carbene hydrogen atoms have been found and refined free. In the asymmetric units cocrystallized molecules of one (**4**), one and a half (**6**, **7b**), or two (**9a**) dichloromethane were included in the models. Both dichloromethane solvent molecules in the structure of **6** are severely disordered. One of these was refined on two positions with a 50:50 occupancy. Another half-occupied, isotropic CH_2Cl_2 was included in the structure model. Several difference peaks in the near proximity indicate a severely disordered second half close by. Severely disordered pentane solvent was included in the molecular structure model of **7b** with an occupancy of 50%. All details and parameters of the measurements are summarized in Table 4.

Acknowledgment. Special thanks to Prof. Dr. H. Fischer for support and discussion. We are indebted to Mr. Galetskiy for recording mass spectra and Ms. Friemel and Mr. Haunz for some of the NMR experiments.

Supporting Information Available: Tables of crystal data, data collection, and refinement parameters, positional and anisotropic displacement parameters, and interatomic distances and angles in CIF format. This material is available free of charge via the Internet at http://pubs.acs.org.

OM8006129

(38) Jaguar, *version 6.0*; Schrödinger, LLC: New York, 2005.

(39) Pennington, W. T. *Diamond*-Crystal and Molecular Structure Visualization Crystal Impact; K. Brandenburg, H. Putz GbR, Postfach 1251, D-53002 Bonn, Germany; for Software Review see:. *J. Appl. Crystallogr.* **1999**, *32*, 1028–1029.

(40) Sheldrick. G. M. *SHELX-97*, Programs for Crystal Structure Analysis; University of Göttingen: Göttingen (Germany), 1997.